Radiative corrections to the neutral-current interactions in the Weinberg-Salam model

S. Sakakibara
Institut für Physik, Universität Dortmund, 4600 Dortmund 50, Federal Republic of Germany
(Received 27 May 1980; revised manuscript received 11 September 1980)

The neutral amplitudes for neutrino-quark scattering are calculated in the one-loop approximation of the standard Weinberg-Salam model of weak and electromagnetic interactions. A careful analysis of renormalization procedure in the 't Hooft–Feynman gauge is presented. Apart from the photonic corrections which are subject to the ordinary QED analysis, purely weak corrections are of the order of one per cent in the amplitudes expressed in terms of the Fermi coupling constant.

I. INTRODUCTION

Since their discovery in 1973, neutral currents have played an important role in the development of particle physics. Numerous investigations of neutral-current interactions established that their structure is remarkably close to the SU(2)×U(1) structure of weak and electromagnetic interactions. In such analyses the neutral-current amplitudes are written in the form of current-current interactions with some coupling parameters that characterize the Lorentz and isospin structure of the currents.[1] The neutral-current parameters are in general arbitrary, but in models of electroweak interactions they are related to each other. In particular, in the sequential Weinberg-Salam model[2] they are functions of only one free parameter $\sin^2\theta$, with θ the Weinberg angle. Various experiments determine the neutral-current parameters or some combinations of them from which $\sin^2\theta$ may be determined. Independent sets of experiments have determined practically the same value $\sin^2\theta \simeq 0.23$, thus giving a firm support for the SU(2)×U(1) structure.[3]

The precise determination of the neutral-current parameters and $\sin^2\theta$ requires careful analysis of radiative corrections which become important as the accuracy of the data improves. Radiative corrections may even provide us with a support for the dynamical aspects of the Weinberg-Salam model in which renormalizability plays an important role. In this paper I calculate radiative corrections to the neutral-current interactions in the standard Weinberg-Salam model with one Higgs doublet. In the tree approximation the neutrino-quark scattering $\nu q \to \nu q$ is described by the Z-exchange diagram in Fig. 1, and the amplitude is given by

$$\frac{-ig^2}{2M_Z^2\cos^2\theta}\bar{\nu}\gamma^\alpha\frac{1-\gamma_5}{2}\nu\bar{q}\gamma_\alpha\left(T_3\frac{1-\gamma_5}{2}-Q\sin^2\theta\right)q\,, \tag{1.1}$$

where T_3 and Q are the weak isospin and electric charge of the quark. The amplitude (1.1) is valid for $|q^2| \ll M_Z^2$, where q is the momentum transfer from the neutrino to the quark. The amplitude (1.1) will receive propagator effects for finite q^2 and radiative corrections from the one-loop diagrams shown in Fig. 2, and the corrected amplitude is represented as

$$\frac{-ig^2}{2M_Z^2\cos^2\theta}\bar{\nu}\gamma^\alpha\frac{1-\gamma_5}{2}\nu\bar{q}\gamma_\alpha \times\left((aT_3+b)\frac{1-\gamma_5}{2}-(cQ-d)\sin^2\theta\right)q\,, \tag{1.2}$$

where a–d are functions of q^2 which are to be computed. Corrections are calculated up to the order α and terms of order $\alpha m_f^2/M_W^2$ in a–d are neglected, where m_f is the fermion mass. The so-called spin terms that have Lorentz structures different from those of (1.2) are also neglected; these terms may contain, for instance, $\bar{q}\sigma_{\alpha\beta}p^\beta q$, where p is an external momentum, and they are smaller than the order α corrections by the factor s/M_W^2 (or t/M_W^2) in the cross section.

It is conventional to express the amplitude (1.1) in terms of the Fermi coupling constant G_F using the relation $G_F/\sqrt{2}=g^2/8M_Z^2\cos^2\theta$. However, since this relation also receives order-α corrections which depend on the renormalization method used, such a replacement in the corrected amplitude (1.2) is in general not allowed. I discuss the corrections to this relation in this paper and express (1.2) in terms of G_F.

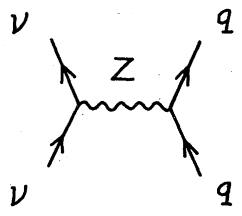

FIG. 1. Born diagram for $\nu q \to \nu q$.

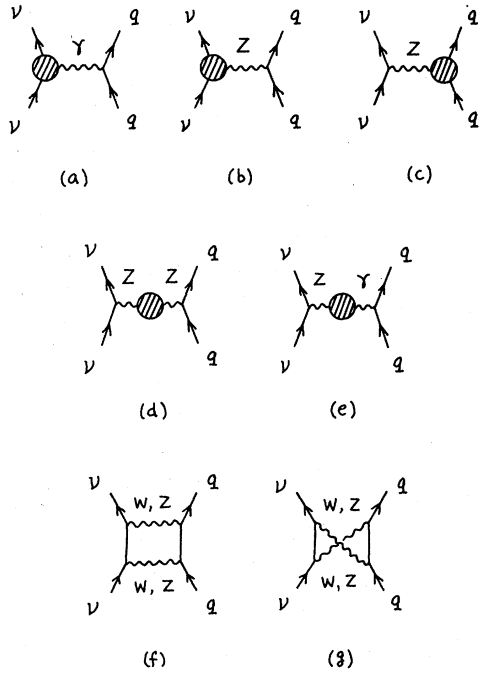

FIG. 2. One-loop corrections to the νq scattering amplitude involving vertex corrections (a)–(c), gauge-meson self-energies (d)–(e) and box diagrams (f)–(g). The shaded blobs represent the sum of all one-loop diagrams.

Calculation of the order-α corrections in the Weinberg-Salam model is not a straightforward task. To extract finite terms from one-loop diagrams, one must distinguish two classes of diagrams: those that are ultraviolet convergent, and those that require the subtraction of appropriate counterterms. In the latter case, it does not suffice to simply throw away divergent terms, since such a procedure is incompatible with the gauge invariance of the theory. In other words, the counterterms correctly determined contain finite terms as well as divergent terms, and the finite terms could give rise to sizable effects. For this reason a large portion of the paper is devoted to a detailed discussion of the subtractions which are consistent with gauge invariance.

The physical picture of the theory is clearest in the so-called U gauge in which the contributions of unphysical fields can be trivially eliminated. In this gauge, however, Green's functions are not well defined since they contain extra divergences that cannot be removed by the renormalization counterterms.[4] Although such extra divergences vanish in the sum of diagrams for an S-matrix element,[5] it is not easy to separate the contribution of each type of the diagrams such as shown in Fig. 2. In the class of R_ξ gauges,[6] all Green's functions are finite after renormalization. Complications in this class of gauges are due to unphysical fields which render the Feynman rules complicated. One may therefore feel that these gauges are not suitable for practical purposes. Fortunately, however, in most cases the contributions of unphysical fields may be neglected. This is because they [the Faddeev-Popov (FP) ghosts] do not couple to fermions or they (the would-be Goldstone bosons) couple to fermions with strength gm_f/M_W, thus contributing only to terms of order $\alpha m_f^2/M_W^2$ which are neglected. The only place where the unphysical fields play an important role is in the gauge-meson self-energies, which is discussed in detail.

Since the full amplitude (1.2) is computed with all the external lines on shell, the results are independent of gauge. I work in the 't Hooft–Feynman gauge[7] in which the symmetry properties of the theory are simplest. In fact in this gauge the vector propagators have the simplest form and, more importantly, all the unphysical propagators have poles at the same locations as the corresponding physical propagators. This enables one to avoid the use of complicated Ward identities; one must simply require that the locations of poles be unchanged by renormalization.

The parameters that characterize the theory are chosen to be

$$(e,\theta,M_W,M_Z,M_H,m_f)\,,$$

the electric charge, the Weinberg angle, W mass, Z mass, Higgs-boson mass, and fermion masses. The Weinberg angle is defined as the mixing angle of the *renormalized* isovector and U(1) gauge fields to form the *renormalized* photon and Z-meson fields [see (2.2)]. Then the renormalized gauge coupling constant g is *defined* by $g=e/\sin\theta$. This definition of g does not contain any ambiguities such as infrared divergences present in other methods.[8,9] I employ the renormalization procedure of Ross and Taylor[10,11] with some modifications; I make the number of parameters minimum so that, for example, I do not introduce the *unrenormalized* Weinberg angle.

The renormalization of the Weinberg-Salam model has been studied by many authors in various gauges.[8-12] One may in principle obtain the necessary counterterms by appropriate redefinitions of the coupling constants and masses in the previous works in Refs. 8–12. However, because of the complexity due to the differences in gauge as well as the subtraction procedure, a direct comparison of the parameters (coupling constants and masses) in the present work and those in Refs. 8–12 is not easy. Therefore, for completeness, all the necessary expressions are presented in this paper.

The plan of the paper is as follows. In Sec. II the Lagrangian is exhibited and the renormalization counterterms are generated. In Secs. III–VI the relevant counterterms and renormalized Green's functions are computed. In particular, in Sec. III the lepton self-energies and the neutrino vertex corrections are computed. The corresponding functions for the quark sector are considered in Sec. IV. Then I proceed in Sec. V to the FP-ghost self-energies which determine the gauge-boson mass counterterms. In Sec. VI the self-energies of the gauge mesons are computed, including the Z-γ transition diagram. In Sec. VII the box diagrams are calculated and the results are presented. In particular, the radiative corrections to the mass ratio M_W/M_Z are discussed. With this result and the radiative corrections to the muon decay amplitude calculated by Ross,[11] the neutral-current amplitudes (1.2) are expressed in terms of the Fermi coupling constant G_F. Appendices A and B contain some of the lengthy expressions. In Appendix C some general features of the radiative corrections in the Weinberg-Salam model are discussed and some aspects that arise in different renormalization procedures are clarified.

II. THE LAGRANGIAN AND THE COUNTERTERMS

The Weinberg-Salam (WS) Lagrangian is written in the manifestly invariant form

$$\mathcal{L}_{\rm WS}=\sum_l i\bar{L}_l\gamma^\mu\left(\partial_\mu-ig\frac{\tau_a}{2}A^a_\mu-i\frac{g'}{2}B_\mu\right)L_l+\sum_l i\bar{R}_l\gamma^\mu(\partial_\mu-ig'B_\mu)R_l-\tfrac{1}{4}F^a_{\mu\nu}F^{a\mu\nu}$$
$$-\tfrac{1}{4}(\partial_\mu B_\nu-\partial_\nu B_\mu)^2+\left|\left(\partial_\mu-ig\frac{\tau_a}{2}A^a_\mu+i\frac{g'}{2}B_\mu\right)\Phi\right|^2-\frac{\lambda}{4}\left(\Phi^\dagger\Phi-\frac{v^2}{2}\right)^2-\sum_l G_l(\bar{L}_l\Phi R_l+\bar{R}_l\Phi^\dagger L_l)+\mathcal{L}_q\,, \tag{2.1}$$

where $F^a_{\mu\nu}=\partial_\mu A^a_\nu-\partial_\nu A^a_\mu+g\epsilon^{abc}A^b_\mu A^c_\nu$. The quark terms $\mathcal{L}_q$ are considered separately in Sec. IV. As usual, the following are defined:

$$\begin{aligned}
W^\pm_\mu&=\frac{1}{\sqrt{2}}(A^1_\mu\mp iA^2_\mu)\,,\\
Z_\mu&=A^3_\mu\cos\theta+B_\mu\sin\theta\,,\\
A_\mu&=-A^3_\mu\sin\theta+B_\mu\cos\theta\,,\\
L_l&=\begin{pmatrix}l_L\\ \nu_l\end{pmatrix}\equiv\frac{1-\gamma_5}{2}\begin{pmatrix}l\\ \nu_l\end{pmatrix}\,,\\
R_l&=l_R\equiv\frac{1+\gamma_5}{2}\,l\,,\\
\Phi&=\begin{pmatrix}\phi^+\\ \frac{1}{\sqrt{2}}(v+\psi+i\chi)\end{pmatrix}\,,
\end{aligned} \tag{2.2}$$

with

$$g\sin\theta=g'\cos\theta=e \tag{2.3}$$

and

$$\begin{aligned}
M_W&=\frac{gv}{2}\,,\\
M_Z&=\frac{gv}{2\cos\theta}\,,\\
M_H{}^2&=\frac{\lambda v^2}{2}\,,\\
m_l&=\frac{G_l v}{\sqrt{2}}\,.
\end{aligned} \tag{2.4}$$

The field ψ is the Higgs scalar of mass M_H. Then (2.1) can be rewritten as

$$\mathcal{L}_{\rm WS}=\sum_l\mathcal{L}_l+\mathcal{L}_{\rm II}+\mathcal{L}_{\rm III}+\mathcal{L}_{\rm IV}+\mathcal{L}_q\,, \tag{2.5}$$

where the explicit expressions are given in Appendix A.

The gauge-fixing terms are chosen in the form[6,7,10]

$$\mathcal{L}_g=-\tfrac{1}{2}(\partial^\mu A_\mu)^2-\left|\partial^\mu W^+_\mu-iM_W\phi^+\right|^2-\tfrac{1}{2}(\partial^\mu Z_\mu-M_Z\chi)^2\,, \tag{2.6}$$

which gives the Goldstone bosons $\phi^\pm,\chi$ (associated with $W^\pm,Z$) masses M_W,M_Z, respectively. Following the usual procedure,[13] the Lagrangian $\mathcal{L}_{\rm FP}$ for the Faddeev-Popov ghosts is obtained (see Appendix A), and we have the effective Lagrangian

$$\mathcal{L}_{\rm eff}=\mathcal{L}_{\rm WS}+\mathcal{L}_g+\mathcal{L}_{\rm FP}\,. \tag{2.7}$$

The Feynman rules can be read off from this Lagrangian, and are listed in Fig. 3 and 4.

So far all the quantities are the bare quantities. The gauge-invariant counterterms are generated by the following transformations:

$$\begin{aligned}
A^a_\mu&\to Z_W{}^{1/2}A^a_\mu\,,\\
B_\mu&\to Z_B{}^{1/2}B_\mu\,,\\
L&\to Z_L{}^{1/2}L\,,\\
R&\to Z_R{}^{1/2}R\,,\\
\Phi&\to Z_\phi{}^{1/2}\Phi\,,\\
g&\to Z_W{}^{-1/2}(g+\delta g)\,,\\
g'&\to Z_B{}^{-1/2}(g'+\delta g')\,,
\end{aligned} \tag{2.8}$$

applied to the Lagrangian (2.1). Here the fields

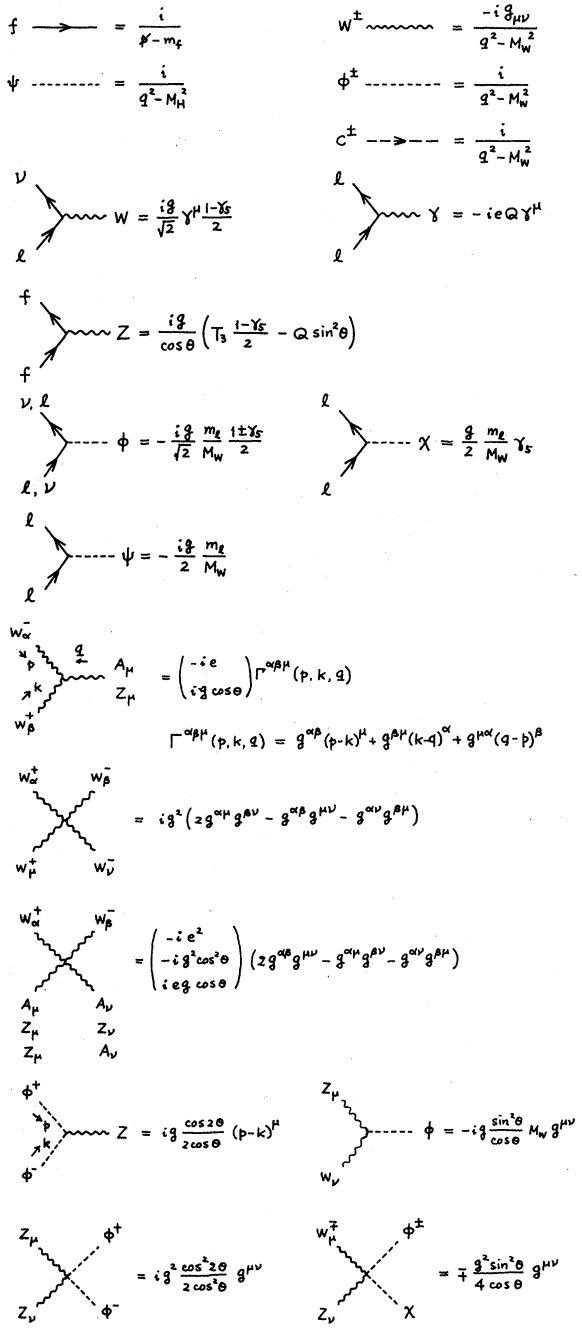

FIG. 3. A partial list of the Feynman rules.

and coupling constants on the right-hand side are the renormalized ones. After these rescalings are performed the resultant Lagrangian is written using (2.2) as the relations among the *renormalized* fields. As for the mass terms, these are written as

$$\mathcal{L}_{\text{mass}}=(Z_\phi M_W{}^2+\delta M_W{}^2)W_\mu^+W^{-\mu}+\tfrac{1}{2}(Z_\phi M_Z{}^2+\delta M_Z{}^2)Z_\mu Z^\mu + \tfrac{1}{2}(Z_\phi M_H{}^2+\delta M_H{}^2)\psi^2-\bar{l}(m_l+\delta m_l)l \qquad (2.9)$$

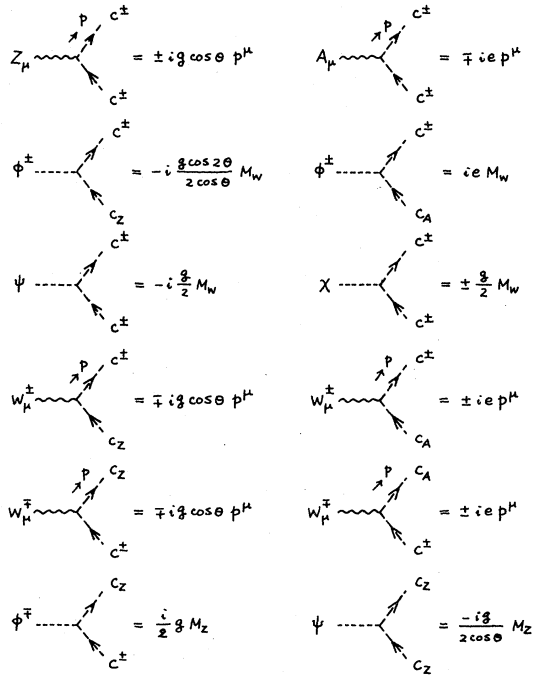

FIG. 4. The complete list of the Feynman rules involving the FP ghosts.

and take M_W, M_Z, M_H, m_l as physical masses measured in experiments. The gauge-meson mass terms are discussed further in Sec. VII. Note that the relations (2.4) are no longer valid after renormalization; they receive one-loop corrections. The resultant Lagrangian is then written as the sum of $\mathcal{L}_{\text{WS}}$ [(2.5), now as the renormalized Lagrangian] and the counterterm Lagrangian $\mathcal{L}^c_{\text{WS}}$. Some relevant terms in $\mathcal{L}^c_{\text{WS}}$ are given in Appendix A. The gauge-fixing terms $\mathcal{L}_g$ given by (2.6) need not be renormalized. However, the gauge transformation for the renormalized fields involves renormalized parameters. Consequently, the FP ghost Lagrangian develops the following counterterms:

$$\mathcal{L}^c_{\text{FP}}=-\delta\tilde{Z}_W\bar{c}^+(\partial^2+M_W{}^2)c^+-\bar{c}^+M_W\delta M_W c^+ - \delta\tilde{Z}_Z\bar{c}_Z(\partial^2+M_Z{}^2)c_Z-\bar{c}_ZM_Z\delta M_Z c_Z+\cdots, \qquad (2.10)$$

where $\tilde{Z}_{W,Z}=1+\delta\tilde{Z}_{W,Z}$ are the wave-function renormalization constants for the ghost fields c^+ and c_Z.

The counterterms involve ultraviolet divergences. To deal with such divergences, the dimensional regularization[14] is used together with the notation

$$\ln\Lambda^2=\frac{2}{4-n}-\gamma+\ln 4\pi\,,$$

where γ is the Euler constant. I assume the sequential model in which the axial-vector anomaly cancels out, and treat γ_5 as anticommuting with all other γ matrices in n dimensions.[15] To deal with the infrared divergences the photon mass δ is introduced. This can be achieved, without destroying gauge invariance, by a spontaneous symmetry breaking, the effects of which vanish as $\delta \to 0$ except for the normal $\log\delta$ in the infrared-divergent terms.[16]

III. THE LEPTON SELF-ENERGIES AND THE NEUTRINO VERTEX FUNCTIONS

The counterterms δg and $\delta g'$ are determined by requiring that the photon vertex function of the lepton defines the physical (renormalized) charge. The charge thus defined must be the same for the electron and muon. This means that δg and $\delta g'$ must be independent of the lepton mass m; otherwise the renormalized charge would be different for the electron and muon, and our renormalization procedure would fail. For this consistency check, all terms involving powers of $m^2/M_W{}^2$ are kept in this section.

Let us first consider the lepton self-energy to determine the lepton wave-function renormalization constants Z_R and Z_L. To determine Z_L we choose to make a subtraction on the neutrino mass shell. Let $-i\nu(p^2)\not{p}(1-\gamma_5)/2$ be the contribution from the one-loop diagrams of Fig. 5(a) and 5(b) to the ν self-energy. The counterterm [Fig. 5(c)] gives, from (A6), the contribution $i\,\delta Z_L \not{p}(1-\gamma_5)/2$, and hence the renormalized ν self-energy is[17]

$$-i\bar{\nu}(p^2)\not{p}\frac{1-\gamma_5}{2} = -i[\nu(p^2)-\delta Z_L]\not{p}\frac{1-\gamma_5}{2}\,. \tag{3.1}$$

The subtraction on the ν mass shell means

$$\frac{1}{\not{p}}[\nu(p^2)-\delta Z_L]\not{p}\frac{1-\gamma_5}{2} \xrightarrow[\not{p}\to 0]{} 0\,,$$

which yields

$$\delta Z_L = \nu(0)\,. \tag{3.2}$$

Before the symmetry breaking, l_L and l_R are two different particles. This is why they carry different renormalization constants Z_L and Z_R. The spontaneous symmetry breaking generates the mass term which mixes l_L and l_R, and we want to treat the mass term as a part of the propagator. Then the propagators for l_L and l_R cannot be separately defined, but one has a single propagator which is a mixture of l_L piece and l_R piece. The l self-energy, coming from the one-loop diagrams [six diagrams similar to Fig. 5(a) and 5(b)], has the structure

$$-i\Sigma(\not{p}) = -i\left(\sigma_L(p^2)\not{p}\frac{1-\gamma_5}{2} + \sigma_R(p^2)\not{p}\frac{1+\gamma_5}{2} + \rho(p^2)m\right). \tag{3.3}$$

Adding the counterterm contribution [Fig. 5(c), with $\nu \to l$] obtained from (A6), the renormalized self-energy is

$$-i\tilde{\Sigma}(\not{p}) = -i\left(\Sigma(\not{p}) - \delta Z_L \not{p}\frac{1-\gamma_5}{2} - \delta Z_R \not{p}\frac{1+\gamma_5}{2} + \delta m\right). \tag{3.4}$$

The mass counterterm δm is discussed in Ref. 9, and we do not consider it here. For the wave-function renormalization constant, we require

$$\frac{1}{\not{p}-m}\tilde{\Sigma}(\not{p}) \xrightarrow[\not{p}\to m]{} f_L\frac{1-\gamma_5}{2} \tag{3.5}$$

which means that the l_R component is subtracted on shell. Since δZ_L has already been determined by (3.2), the number f_L cannot be zero, but is finite. The condition (3.5) fixes δZ_R and f_L as

$$\delta Z_R = \sigma_{R0} + 2\sigma_{R1} + 2\rho_1\,, \tag{3.6}$$

$$f_L = \sigma_{L0} + 2\sigma_{L1} + 2\rho_1 - \delta Z_L\,, \tag{3.7}$$

where σ_i, ρ_i are the coefficients of the expansion of $\sigma(p^2)$, $\rho(p^2)$ about $p^2 = m^2$,

$$\begin{aligned}\sigma_{R,L}(p^2) &= \sigma_{R,L} + \sigma_{R,L1}\frac{p^2-m^2}{m^2} + \cdots,\\ \rho(p^2) &= \rho_0 + \rho_1\frac{p^2-m^2}{m^2} + \cdots.\end{aligned} \tag{3.8}$$

The f_L is a constant remaining after renormalization, and a factor $\frac{1}{2}f_L(1-\gamma_5/2)$ is to be associated to each (renormalized) external l line. ($\frac{1}{2}f_L$, because the renormalization constant for an external line is $Z_L{}^{1/2} \simeq 1 + \frac{1}{2}\delta Z_L$ but not Z_L).

Calculation of each diagram in Figs. 5(a) and 5(b) gives

$$\begin{aligned}\nu(p^2)^W &\doteq -\tfrac{1}{2}\ln\frac{\Lambda^2}{M_W{}^2} + \frac{1}{2} + I_1(M_W, m, p)\,,\\ \nu(p^2)^Z &\doteq \frac{-1}{2\cos^2\theta}\left[\frac{1}{2}\ln\frac{\Lambda^2}{M_Z{}^2} - \frac{1}{2} - I_1(M_Z, 0, p)\right],\\ \nu(p^2)^\Phi &\doteq -\frac{m^2}{M_W{}^2}\left[\frac{1}{4}\ln\frac{\Lambda^2}{M_W{}^2} - \tfrac{1}{2}I_1(M_W, m, p)\right],\\ I_1(M, m, p) &\doteq \int_0^1 dx(1-x)\ln\left[1 - x + x\frac{m^2}{M^2} - x(1-x)\frac{p^2}{M^2}\right].\end{aligned} \tag{3.9}$$

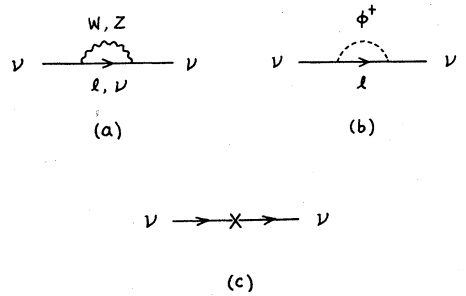

FIG. 5. Diagrams contributing to the neutrino self-energy.

Here and below, the symbol $\doteq$ means that the right-hand side must be multiplied by the common factor $g^2/16\pi^2$. From (3.2), we obtain

$$\delta Z_L^W \doteq -\frac{1}{2}\ln\frac{\Lambda^2}{M_W^2}+\frac{1}{2}+I_1(M_W,m,0),$$

$$\delta Z_L^Z \doteq \frac{-1}{2\cos^2\theta}\left(\frac{1}{2}\ln\frac{\Lambda^2}{M_Z^2}-\frac{1}{4}\right),$$

$$\delta Z_L^\phi \doteq -\frac{m^2}{M_W^2}\left[\frac{1}{4}\ln\frac{\Lambda^2}{M_W^2}-\frac{1}{2}I_1(M_W,m,0)\right]$$

$$\delta Z_L = \delta Z_L^W+\delta Z_L^Z+\delta Z_L^\phi. \tag{3.10}$$

The quantities ρ and σ can be calculated from the one-loop diagrams [Figs. 5(a) and 5(b), with $\nu \to l$], from which and from (3.6) we find

$$\delta Z_R^Z \doteq \frac{2\sin^4\theta}{\cos^2\theta}\left[-\frac{1}{2}\ln\frac{\Lambda^2}{M_Z^2}+\frac{1}{2}+I_2(M_Z,m,m)-2\frac{m^2}{M_Z^2}\int_0^1 dx\,\frac{x(1-x)^2}{1-x+x^2(m^2/M_Z^2)}\right]$$
$$-\frac{4\sin^2\theta\cos2\theta}{\cos^2\theta}\frac{m^2}{M_Z^2}\int_0^1 dx\,\frac{x(1-x)}{1-x+x^2(m^2/M_Z^2)},$$

$$\delta Z_R^\gamma \doteq -\sin^2\theta\left(\ln\frac{\Lambda^2}{m^2}+4+2\ln\frac{\delta^2}{m^2}\right), \tag{3.11}$$

$$I_2(M,m,p)=\int_0^1 dx(1-x)\ln\left[(1-x)\left(1-x\frac{p^2}{M^2}\right)+x\frac{m^2}{M^2}\right].$$

All other contributions, δZ_R^ϕ, δZ_R^χ, δZ_R^ψ, can be obtained similarly. It is convenient to deal with the constant f_L, defined in (3.7), in groups as

$$f_L^W+\delta Z_L^W \doteq -\frac{1}{2}\ln\frac{\Lambda^2}{M_W^2}+\frac{1}{2}+I_2(M_W,0,m)-2\frac{m^2}{M_W^2}\int_0^1 dx\,\frac{x(1-x)}{1-x(m^2/M_W^2)},$$

$$f_L^Z+f_L^\gamma+\delta_L^Z \doteq \frac{\cos^2 2\theta}{4\cos^2\theta}\left[-\ln\frac{\Lambda^2}{M_Z^2}+1+2I_2(M_Z,m,m)-4\frac{m^2}{M_Z^2}\int_0^1 dx\,\frac{x(1-x)^2}{1-x+x^2(m^2/M_Z^2)}\right] \tag{3.12}$$
$$-\frac{4\sin^2\theta\cos2\theta}{\cos^2\theta}\frac{m^2}{M_Z^2}\int_0^1 dx\,\frac{x(1-x)}{1-x+x^2(m^2/M_Z^2)}-\sin^2\theta\left(\ln\frac{\Lambda^2}{m^2}+4+2\ln\frac{\delta^2}{m^2}\right),$$

and similarly for $f_L^\chi+f_L^\phi+\delta Z_L^\phi$. Then from (3.10) we see that the divergences cancel in each group and f_L becomes finite,

$$f_L=\frac{e^2}{16\pi^2}\left(-\ln\frac{M_Z^2}{m^2}-\frac{9}{2}-2\ln\frac{\delta^2}{m^2}\right)+O\left(\alpha\frac{m^2}{M_W^2}\right), \tag{3.13}$$

where only the leading terms are exhibited.

The lepton-photon vertex corrections depicted by the diagrams in Figs. 6(a)–6(f) are now calculated. In the limit of $q^2 \to 0$ (q is the photon momentum), the contribution from these diagrams can be written as

$$ie\gamma^\mu\frac{1-\gamma_5}{2}\Lambda_L+ie\gamma^\mu\frac{1+\gamma_5}{2}\Lambda_R, \tag{3.14}$$

where $\Lambda_{L,R}$ are constants which we are to compute. Let us begin with the Z-exchange diagram in Fig. 6(d). With some algebra we find

$$\Lambda_R^Z \doteq \frac{2\sin^4\theta}{\cos^2\theta}\left[\frac{1}{2}\ln\frac{\Lambda^2}{M_Z^2}-1-\int_0^1 dx\,x\ln\left(1-x+x^2\frac{m^2}{M_Z^2}\right)+\frac{m^2}{M_Z^2}\int_0^1 dx\,\frac{x(1-x)^2+x}{1-x+x^2(m^2/M_Z^2)}\right].$$
$$+\frac{4\sin^2\theta\cos2\theta}{\cos^2\theta}\frac{m^2}{M_Z^2}\int_0^1 dx\,\frac{x(1-x)}{1-x+x^2(m^2/M_Z^2)}. \tag{3.15}$$

Quite remarkably, at least from the appearance of the expressions, one can verify with some manipulations that the sum $\delta Z_R^Z+\Lambda_R^Z$ vanishes. We have checked such cancellations for other contributions, and have found that $\delta Z_R^A+\Lambda_R^A=0$, $A=(Z,\gamma,\phi,\chi,\psi)$. Collecting all these, we find

$$\delta Z_R+\Lambda_R=0, \tag{3.16}$$

which is valid to all orders in m^2/M_W^2.

Let us now compute the W-exchange diagram. It is convenient to group three diagrams in Figs. 6(a)–6(c) together, whose contribution is given by

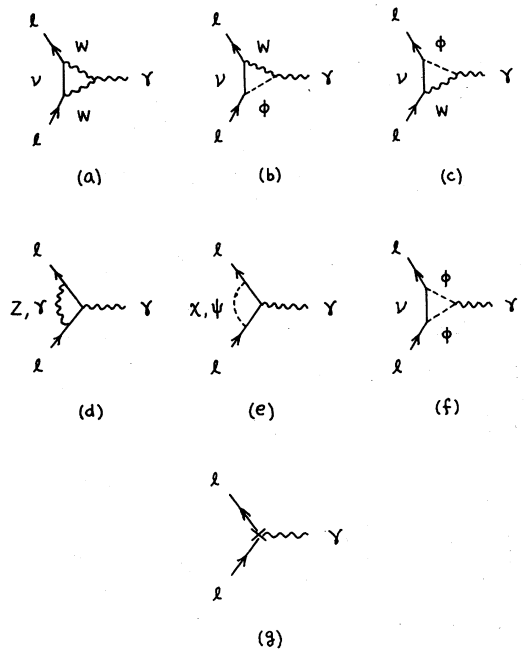

FIG. 6. One-particle irreducible diagrams contributing to the lepton-photon vertex.

$$\Lambda_L^W \doteq \tfrac{3}{2}\ln\frac{\Lambda^2}{M_W^2} - \frac{1}{2} - I_2(M_Z, 0, m) + 2\frac{m^2}{M_W^2}\int_0^1 dx\,\frac{x(1-x)}{1-x(m^2/M_W^2)}\,. \tag{3.17}$$

It is obvious from (3.12) and (3.17) that $f_L^W + \delta Z_L^W + \Lambda_L^W \doteq \ln(\Lambda^2/M_W^2)$. For the contributions from other diagrams in Fig. 6(d)–6(f), I have checked that $f_L^Z + f_L^\gamma + \delta Z_L^Z + \Lambda_L^Z + \Lambda_L^\gamma = 0$ and $f_L^\chi + f_L^\psi + \delta Z_L^\phi + \Lambda_L^\chi + \Lambda_L^\psi = 0$. Summing all these terms yields

$$f_L + \delta Z_L + \Lambda_L = \frac{g^2}{16\pi^2}\ln\frac{\Lambda^2}{M_W^2}\,. \tag{3.18}$$

I emphasize again that this equation is valid to all orders in m^2/M_W^2.

Finally the contribution from the counterterms, Fig. 6(g) is considered. Using the same notation as in (3.14), from (A.6) it is found that

$$\Lambda_R^c = \delta Z_R + \frac{\delta g'}{e}\cos\theta\,, \qquad \Lambda_L^c = \delta Z_L + \frac{\delta g}{2g} + \frac{\delta g'}{2g}\cot\theta\,. \tag{3.19}$$

We now have all the terms necessary to determine δg and $\delta g'$. Consider all the contributions to the photon vertex up to the order g^3, with the lepton on shell. They are the diagrams shown in Fig. 7, where each shaded blob represents the sum of all one-loop diagrams and the counterterms (i.e., the renormalized two- and three-point functions of order g^2). We impose the usual renormalization condition; the sum of these diagrams approaches

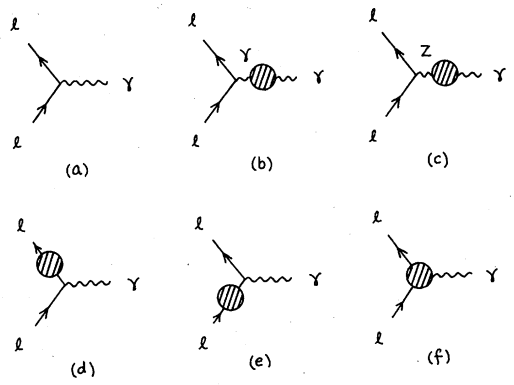

FIG. 7. Diagrams contributing to the lepton-photon vertex. The shaded blobs represent renormalized two- and three-point functions of order α.

$ie\gamma^\nu$ as $q^2 \to 0$, which is already given by the tree diagram Fig. 7(a). Therefore, the sum of all the corrections must vanish. As shall be discussed in later sections, the photon self-energy is subtracted on shell of the photon. Thus the diagram of Fig. 7(b) vanishes as $q^2 \to 0$ [see (6.2)]. It will also be seen later that the Z-γ transition diagram in Fig. 7(c) vanishes as $q^2 \to 0$ [see (6.24)]. According to the rule for external lines, the diagrams of Figs. 7(d) and 7(e) give $\frac{1}{2} f_L ie\gamma^\mu(1-\gamma_5/2)$. For the diagram of Fig. 7(f), the sum of (3.14) and (3.19) is obtained. Thus our renormalization condition requires

$$\Lambda_R + \delta Z_R + \frac{\delta g'}{e}\cos\theta = 0\,, \qquad f_L + \Lambda_L + \delta Z_L + \frac{\delta g}{2g} + \frac{\delta g'}{2g}\cot\theta = 0\,. \tag{3.20}$$

Then, together with (3.16) and (3.18), we find

$$\delta g' = 0\,, \qquad \delta g = -\frac{2g^3}{16\pi^2}\ln\frac{\Lambda^2}{M_W^2}\,. \tag{3.21}$$

This result is valid to all orders in m^2/M_W^2. If δg and/or $\delta g'$ had depended on the lepton mass, then the renormalized charge of the electron and muon would be different, since the same δg and $\delta g'$ are subtracted at the $ee\gamma$ vertex as well as at the $\mu\mu\gamma$ vertex.

Once the counterterms (3.21) are found, the coupling of the neutrino to the photon, which is induced by the diagrams in Fig. 8, can be computed. The counterterm Fig. 8(e) is given from (A.6) by

$$-i\frac{\delta g}{2}\sin\theta\,\gamma^\mu\,\frac{1-\gamma_5}{2} \tag{3.22}$$

with δg given by (3.21), which cancels the divergence arising from Figs. 8(a)–8(d), leaving the finite result

$$ie\gamma^{\mu}\frac{1-\gamma_5}{2}\frac{g^2}{16\pi^2}\tilde{\Lambda}_{\nu}(q^2), \tag{3.23}$$

where

$$\tilde{\Lambda}_{\nu}(q^2) = -\tfrac{1}{2} - \int_0^1 dx \int_0^{1-x} dy \ln\left(1-x-y+(x+y)\frac{m^2}{M_W{}^2} - xy\frac{q^2}{M_W{}^2}\right)$$

$$+\frac{1}{M_W{}^2}\int_0^1 dx \int_0^{1-x} dy \frac{(1-x)(1-y)q^2+m^2}{1-x-y+(x+y)(m^2/M_W{}^2)-xy(q^2/M_W{}^2)}$$

$$+\int_0^1 dx \int_0^{1-x} dy \ln\left(x+y+(1-x-y)\frac{m^2}{M_W{}^2} - xy\frac{q^2}{M_W{}^2}\right)$$

$$+\int_0^1 dx \int_0^{1-x} dy \frac{(x+y)(q^2/M_W{}^2)}{x+y+(1-x-y)(m^2/M_W{}^2)-xy(q^2/M_W{}^2)} + \int_0^1 dx \ln\left(1-x(1-x)\frac{q^2}{M_W{}^2}\right). \tag{3.24}$$

For small $|-q^2|$ compared with $M_W{}^2$, one can expand (3.24) in powers of $q^2/M_W{}^2$. Keeping terms involving the ratio q^2/m^2,

$$\tilde{\Lambda}_{\nu} = \frac{-q^2}{M_W{}^2}\left[-\frac{1}{3}+\frac{1}{3}\ln\frac{m^2}{M_W{}^2}+2\int_0^1 dx\, x(1-x)\ln\left(1-x(1-x)\frac{q^2}{m^2}\right)\right]. \tag{3.25}$$

For very small $|-q^2| \ll m^2$,

$$\tilde{\Lambda}_{\nu} \simeq \frac{-q^2}{M_W{}^2}\left(-\frac{1}{3}+\frac{1}{3}\ln\frac{m^2}{M_W{}^2}+\frac{1}{15}\frac{-q^2}{m^2}\right). \tag{3.26a}$$

Thus for very small $-q^2$ the lepton mass gives the dominant effect; $\ln(M_W{}^2/m_e{}^2) \simeq 24$ and $\ln(M_W{}^2/m_{\mu}{}^2) \simeq 14$. Consequently, for very small $|-q^2|$ $\tilde{\Lambda}_{\nu}$ is considerably different for ν_{μ} and ν_e. This difference gives rise to the apparent ν_{μ}-ν_e universality violation in neutral-current interactions.[18] For $m^2 \ll -q^2 \ll M_W{}^2$,

$$\tilde{\Lambda}_{\nu}(q^2) \simeq \frac{-q^2}{M_W{}^2}\left(-\frac{8}{9}+\frac{1}{3}\ln\frac{-q^2}{M_W{}^2}\right), \tag{3.26b}$$

which is a good approximation already for $-q^2/m^2 \simeq 100$.[19] Thus the fermion mass effects rapidly disappear as $-q^2$ increases. In other words, the fermion mass simply serves as an infrared cutoff. The contribution of this term to the amplitude (1.2) corresponding to Fig. 2(a), which is denoted with subscript 2(a), is

$$c_{2(a)} = -\frac{g^2}{16\pi^2}2\frac{M_W{}^2}{q^2}\tilde{\Lambda}_{\nu}(q^2) \tag{3.27}$$

and $a=b=d=0$.

The corrections to the $\nu\nu Z$ vertex arise from the diagrams in Figs. 8(a), 8(d), and 8(e) with the replacement $\gamma \to Z$. There is also a diagram of the type Fig. 8(d) with the exchange of Z in place of W. Subtracting the counterterms

$$\left(\frac{ig}{2\cos\theta}\delta Z_L + \frac{i\delta g}{2}\cos\theta\right)\gamma^{\mu}\frac{1-\gamma_5}{2}, \tag{3.28}$$

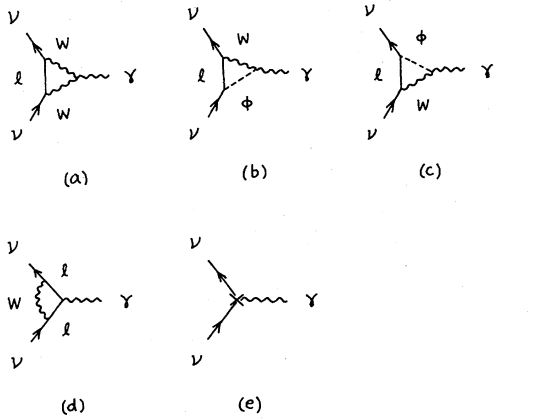

FIG. 8. One-particle irreducible diagrams contributing to the induced neutrino-photon vertex.

where δZ_L and δg are given by (3.10) and (3.21), we find for the $\nu\nu Z$ vertex correction

$$\frac{ig}{2\cos\theta}\gamma^\mu\frac{1-\gamma_5}{2}\frac{g^2}{16\pi^2}\tilde{\Lambda}_Z(q^2), \tag{3.29}$$

where

$$\tilde{\Lambda}_Z=\frac{-1}{2\cos^2\theta}I_3(q,M_Z)+(1-2\sin^2\theta)I_3(q,M_W) - 2\cos^2\theta\, I_4(q,M_W{}^2), \tag{3.30a}$$

$$I_3(q,M)=\int_0^1 dx\int_0^{1-x}dy\,\ln\left(1-\frac{xy}{1-x-y}\frac{q^2}{M^2}\right),$$

$$I_4(q,M)=\int_0^1 dx\ln\left(1-x(1-x)\frac{q^2}{M^2}\right) +\int_0^1 dx\int_0^{1-x}dy\ln\left(1-\frac{xy}{x+y}\frac{q^2}{M^2}\right) +\frac{q^2}{M^2}\int_0^1 dx\int_0^{1-x}dy\frac{x+y}{x+y-xy(q^2/M^2)} \tag{3.30b}$$

The contribution of (3.29) to the amplitude (1.2) corresponding to Fig. 2(b) is

$$a_{2(b)}(q^2)=c_{2(b)}(q^2)=\frac{g^2}{16\pi^2}\frac{\tilde{\Lambda}_Z(q^2)}{1-(q^2/M_Z{}^2)} \tag{3.31}$$

and $b=d=0$. Here we have neglected terms of order $\alpha m^2/M_W{}^2$.

IV. THE QUARK CONTRIBUTIONS

For simplicity only the u and d quarks are considered. The Lagrangian $\mathcal{L}_q$ for the quarks can be written down in the same way as for the leptons[20] and we do not bother to exhibit it here. The left-handed quarks form a doublet (u_L, d_L) while the right-handed quarks are two singlets, u_R and d_R. Correspondingly, there are three independent wave-function renormalization constants $\bar{Z}_L$, $\bar{Z}_u$, and $\bar{Z}_d$. In terms of these constants, the counter-term Lagrangian involving the Z meson and photon becomes

$$\mathcal{L}_q^c=\sum_q\left[\left(\delta\bar{Z}_L\frac{g}{\cos\theta}(T_3-Q\sin^2\theta)+\delta g T_3\cos\theta\right)Z_\mu - (\delta\bar{Z}_L Qg\sin\theta+\delta g T_3\sin\theta)A_\mu\right]\bar{q}_L\gamma^\mu q_L - \sum_q\delta\bar{Z}_q Qg\sin\theta(Z_\mu\tan\theta+A_\mu)\bar{q}_R\gamma^\mu q_R. \tag{4.1}$$

The subtraction for the u-quark self-energy is made on shell. Thus we find $\delta\bar{Z}_L=\delta\bar{Z}_L^W+\delta\bar{Z}_L^Z+\delta\bar{Z}_L^\gamma$,

$$\delta\bar{Z}_L^W\doteq-\frac{1}{2}\ln\frac{\Lambda^2}{M_W{}^2}+\frac{1}{4},$$

$$\delta\bar{Z}_L^Z\doteq\frac{1}{\cos^2\theta}\left(\frac{1}{2}-\frac{2}{3}\sin^2\theta\right)^2\left(-\ln\frac{\Lambda^2}{M_Z{}^2}+\frac{1}{2}\right), \tag{4.2}$$

$$\delta\bar{Z}_L^\gamma\doteq-\tfrac{4}{9}\sin^2\theta\left(\ln\frac{\Lambda^2}{m_q{}^2}+4+2\ln\frac{\delta^2}{m_q{}^2}\right).$$

The Higgs-boson contribution is negligible. Since the d-quark self-energy is not subtracted on shell, a finite constant $\bar{f}_L$ remains on shell of d as

$$\frac{1}{\not p-m_d}\tilde{\Sigma}_d(\not p)\xrightarrow[\not p\to m_d]{}\bar{f}_L\frac{1-\gamma_5}{2} \tag{4.3}$$

By the similar procedure as in Sec. III [Eqs. (3.5)–(3.13)], we find

$$\delta\bar{Z}_q^W=0,$$

$$\delta\bar{Z}_q^Z\doteq Q^2\frac{\sin^4\theta}{\cos^2\theta}\left(-\ln\frac{\Lambda^2}{M_Z{}^2}+\frac{1}{2}\right),$$

$$\delta\bar{Z}_q^\gamma\doteq-Q^2\sin^2\theta\left(\ln\frac{\Lambda^2}{m_q{}^2}+4+2\ln\frac{\delta^2}{m_q{}^2},\right) \tag{4.4}$$

$$\bar{f}_L\doteq\tfrac{1}{3}\sin^2\theta\left(\ln\frac{M_Z{}^2}{m_q{}^2}+\frac{9}{2}+2\ln\frac{\delta^2}{m_q{}^2}\right).$$

The one-loop diagrams contributing to the qqZ vertex are essentially the same as those for the $\nu\nu Z$ vertex. The only difference is the presence of the photon-exchange diagram as well as the factor of $\frac{1}{2}\bar{f}_L$ for each external d line. Calculation gives the result

$$\frac{ig}{\cos\theta}\frac{g^2}{16\pi^2}\tilde{\Lambda}^\mu_{qqZ}(q^2), \tag{4.5}$$

where, excluding the contribution of the photon-exchange diagram,

$$\tilde{\Lambda}^\mu_{qqZ}=[T_3-(Q-\tfrac{1}{3})\sin^2\theta]\gamma^\mu\frac{1-\gamma_5}{2}I_3(q,M_W) - \frac{2\gamma^\mu}{\cos^2\theta}\left((T_3-Q\sin^2\theta)^3\frac{1-\gamma_5}{2}-(Q\sin^2\theta)^3\frac{1+\gamma_5}{2}\right)I_3(q,Mz)-2\cos^2\theta T_3\gamma^\mu\frac{1-\gamma_5}{2}I_4(q,Mw) \tag{4.6}$$

with $I_{3,4}$ defined in (3.30b). It is convenient to write the photon-exchange contribution separately as

$$Q^2\sin^2\theta\left[2\ln\frac{\delta^2}{m^2}\left(\ln\frac{-q^2}{m_q{}^2}-1\right)-\ln^2\frac{-q^2}{m_q{}^2}\right]\cdot T_{\text{tree}}, \tag{4.7}$$

where T_{tree} stands for the tree amplitude (1.1), and I have assumed that $-q^2\gg m_q{}^2$. The contribution of (4.5) to the amplitude (1.2) corresponding to Fig. 2(c), $a_{2(c)}-d_{2(c)}$, can be read off from (4.6).

V. THE SELF-ENERGIES FOR THE FADDEEV-POPOV GHOSTS

We now proceed to the gauge-meson sector, and determine δM_W^2, δM_Z^2, Z_W, and Z_B. It appears at first that one can do the usual subtraction, i.e., subtract on mass shell of $W^\pm$ and Z, thus determining the four constants. We note, however, that the photon does not carry an independent wave-function renormalization constant. Therefore, one is then no longer allowed to subtract on shell of the photon. A consequence of this would be that the diagram of Fig. 7(b) does not vanish as $q^2 \to 0$, which drastically complicates the determination of δg. Furthermore, the above subtraction is not *a priori* gauge invariant, since various Green's functions are related by Ward identities, and such subtractions would destroy these relations after renormalization. Thus we require two conditions: (1) subtract the photon self-energy on shell of the photon, and (2) make subtraction in accordance with Ward identities. To satisfy these conditions, the calculation of the ghost self-energies becomes necessary.

There exists one FP ghost field for each gauge vector field. Thus there are four FP ghosts $c^\pm$, c_Z, c_A, in the WS theory. Although in certain gauges c_A completely decouples, in our gauge defined by (2.6) all of them are important entities. However, in this section the self-energies of $c^\pm$ and c_Z are calculated, but not that of c_A, for this is done only to calculate the gauge-boson mass counterterms $\delta M_W{}^2$ and $\delta M_Z{}^2$. The self-energy functions themselves are not needed for our purposes since they begin to appear at the two-loop level.

Let $ie^W(q^2)$ $[ie^Z(q^2)]$ be the sum of all one-loop contributions to the c^+ $[c_Z]$ self-energy, Figs. 9(a) and 9(b) [similar diagrams for c_Z]. The counterterm contribution, Fig. 9(c), is $i\delta\tilde{Z}_W(q^2 - M_W{}^2) - iM_W\delta M_W$ $[i\delta\tilde{Z}_Z(q^2 - M_Z{}^2) - iM_Z\delta M_Z]$ obtained from (2.10). Thus the renormalized self-energies are $i\tilde{e}^W(q^2)$ and $i\tilde{e}^Z(q^2)$,

$$\begin{aligned} \tilde{e}^W(q^2) &= e^W(q^2) + \delta\tilde{Z}_W(q^2 - M_W{}^2) - M_W\delta M_W , \\ \tilde{e}^Z(q^2) &= e^Z(q^2) + \delta\tilde{Z}_Z(q^2 - M_Z{}^2) - M_Z\delta M_Z . \end{aligned} \tag{5.1}$$

Due to gauge invariance of the theory, $\tilde{e}^W(q^2)$ is related to the self-energy of W^+ by Ward identity. Therefore the renormalization condition for $\tilde{e}^W(q^2)$ must be compatible with the Ward identity. This is the point where the 't Hooft–Feynman gauge provides us an advantage. In this gauge, the FP ghosts $c^\pm$ and c_Z, as well as the Goldstone fields $\phi^\pm$ and χ, are nothing but the longitudinal components of the corresponding gauge vector mesons

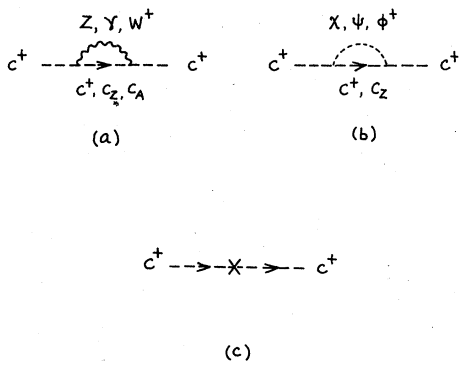

FIG. 9. Diagrams contributing to the FP ghost c^+ self-energy.

$W^\pm$ and Z.[21] This is why their propagators have poles at the same point as the vector-meson propagators: at $q^2 = M_W{}^2$ for $c^\pm$, and at $q^2 = M_Z{}^2$ for c_Z. These locations of poles have to be maintained after renormalization. Thus we have the following simple conditions:

$$\begin{aligned} &\tilde{e}^W(M_W{}^2) = 0 , \\ &\tilde{e}^Z(M_Z{}^2) = 0 , \end{aligned} \tag{5.2}$$

which give $e^W(M_W{}^2) = M_W\delta M_W$, etc. Since $2M_W\delta M_W = \delta M_W{}^2$, we write

$$\begin{aligned} \delta M_W{}^2 &= 2e^W(M_W{}^2) , \\ \delta M_Z{}^2 &= 2e^Z(M_Z{}^2) . \end{aligned} \tag{5.3}$$

At this point, it may help to remark on some peculiar features of the ghost Feynman rules in Fig. 4. First of all, we note that the ghosts c^+ and c^- are two different fields. This means that the c^+ loop and the c^- loop must be counted separately, in contrast to a $W^\pm$ loop which is counted only once. This is because W^- is the antiparticle of W^+, while the antiparticle of c^+ is not c^-.[22] The second remark is that the FP ghosts are fermions and one must keep track of the arrows in their propagators. In particular, there is no vertex for $c^+ \to c_A + \phi^+$, although the vertex exists for $c_A + \phi^+ \to c^+$. Therefore a diagram such as shown in Fig. 10 does not exist. Furthermore, there are vertices for $c_Z \to c^+ + \phi^-$ and $c^+ + \phi^- \to c_Z$, but they carry different coupling strengths.

With these remarks, actual calculation of the diagrams in Fig. 9 is straightforward. We merely write down the results:

$$\frac{\delta M_W^2}{M_W^2}=\frac{g^2}{16\pi^2}\left[\left(\tfrac{1}{2}\tan^2\theta-\tfrac{5}{2}\right)\ln\frac{\Lambda^2}{M_W^2}-4\sin^2\theta+\left(3-\tfrac{1}{2}\tan^2\theta+2\sin^2\theta\right)\int_0^1 dx\ln\left(x^2+(1-x)\frac{M_Z^2}{M_W^2}\right)\right.$$
$$\left.-\tfrac{1}{2}\int_0^1 dx\ln\left(x^2+(1-x)\frac{M_H^2}{M_W^2}\right)\right],$$
$$\frac{\delta M_Z^2}{M_Z^2}=\frac{g^2}{16\pi^2}\left[\left(4\sin^2\theta+\tfrac{1}{2}\tan^2\theta-\tfrac{5}{2}\right)\ln\frac{\Lambda^2}{M_W^2}+\left(3-4\sin^2\theta\right)\int_0^1 dx\ln\left(1-x(1-x)\frac{M_Z^2}{M_W^2}\right)\right.$$
$$\left.-\frac{1}{2\cos^2\theta}\int_0^1 dx\ln\left(x^2\frac{M_Z^2}{M_W^2}+(1-x)\frac{M_H^2}{M_W^2}\right)\right] \tag{5.4}$$

VI. GAUGE-MESON SELF-ENERGIES

In this section, we compute the self-energies for the gauge mesons, and determine the wave-function renormalization constants Z_W and Z_B. To this end, we first compute the photon self-energy coming from all the one-loop diagrams in Figs. 11(a)–11(g), which we denote by $i\pi^\gamma(q^2)(q^2g_{\mu\nu}-q_\mu q_\nu)$. From (A6) the counterterm contribution [Fig. 11(h)] is $-i(\delta Z_W\sin^2\theta+\delta Z_B\cos^2\theta)(q^2g_{\mu\nu}-q_\mu q_\nu)$, so that the renormalized photon self-energy is

$$i\tilde\pi^\gamma_{\mu\nu}(q^2)=i\pi^\gamma(q^2)(q^2g_{\mu\nu}-q_\mu q_\nu)\,,$$
$$\tilde\pi^\gamma(q^2)=\pi^\gamma(q^2)-(\delta Z_W\sin^2\theta+\delta Z_B\cos^2\theta)\,. \tag{6.1}$$

As we have discussed in the previous section, we treat the photon in the usual way, i.e., make subtraction on shell,

$$\tilde\pi^\gamma(q^2)\xrightarrow[q^2\to0]{}0\,. \tag{6.2}$$

Thus we find

$$\delta Z_W\sin^2\theta+\delta Z_B\cos^2\theta=\pi^\gamma(0)\,. \tag{6.3}$$

Next we compute the Z and $W^\pm$ self-energies, coming from all the one-loop diagrams (similar to those in Fig. 11), which we write as

$$i\pi^{Z,W}_{\mu\nu}(q^2)=ia^{Z,W}(q^2)\left(g_{\mu\nu}-\frac{q_\mu q_\nu}{q^2}\right)$$
$$+ib^{Z,W}(q^2)\frac{q_\mu q_\nu}{q^2}\,. \tag{6.4}$$

From (A6) the counterterm contributions are $-i\delta Z_{Z,W}(q^2g_{\mu\nu}-q_\mu q_\nu)+i(\delta Z_\phi M_{Z,W}^2+\delta M_{Z,W}^2)g_{\mu\nu}$ with the notation

$$\delta Z_Z=\delta Z_W\cos^2\theta+\delta Z_B\sin^2\theta\,. \tag{6.5}$$

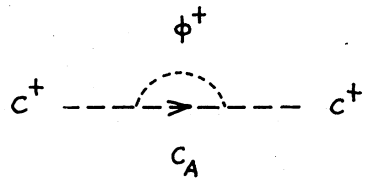

FIG. 10. An example of diagrams which do *not* exist in our Feynman rules.

Then the renormalized Z and $W^\pm$ self-energies are

$$i\tilde\pi^{Z,W}_{\mu\nu}(q^2)=i\tilde a^{Z,W}(q^2)g_{\mu\nu}+i\tilde b^{Z,W}(q^2)\frac{q_\mu q_\nu}{q^2}\,, \tag{6.6a}$$

$$\tilde a^{Z,W}(q^2)=a^{Z,W}(q^2)-\delta Z_{Z,W}q^2$$
$$+\delta Z_\phi M_{Z,W}^2+\delta M_{Z,W}^2\,. \tag{6.6b}$$

Now in our gauge (2.6), the relevant Ward identity reduces to the statement that the renormalized propagators must maintain the poles at $q^2=M_{Z,W}^2$. It follows from (6.6) that

$$\tilde a^{Z,W}(M_{Z,W}^2)=0\,, \tag{6.7}$$

which in turn gives rise to the equations

$$\frac{a^{Z,W}(M_{Z,W}^2)}{M_{Z,W}^2}-\delta Z_{Z,W}+\delta Z_\phi+\frac{\delta M_{Z,W}^2}{M_{Z,W}^2}=0\,. \tag{6.8}$$

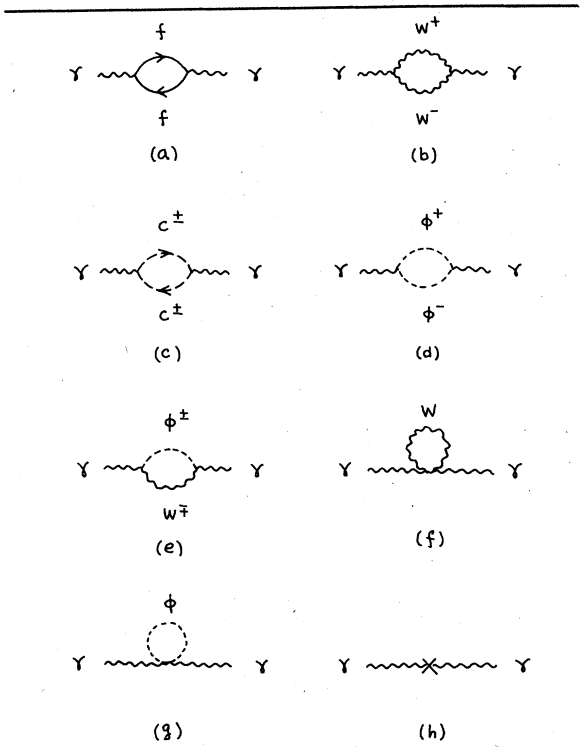

FIG. 11. Diagrams contributing to the photon self-energy.

By eliminating δZ_ϕ from (6.8), we obtain

$$Y_{WZ} = \delta Z_W - \delta Z_Z = (\delta Z_W - \delta Z_B)\sin^2\theta\,, \tag{6.9}$$

where we have defined

$$Y_{WZ} = \frac{a^W(M_W^2)}{M_W^2} - \frac{a^Z(M_Z^2)}{M_Z^2} + \frac{\delta M_W^2}{M_W^2} - \frac{\delta M_Z^2}{M_Z^2}. \tag{6.10}$$

Finally, from (6.3) and (6.9), we find

$$\begin{aligned} \delta Z_B &= \pi^\gamma(0) - Y_{WZ}\,, \\ \delta Z_W &= \pi^\gamma(0) + Y_{WZ}\cot^2\theta\,. \end{aligned} \tag{6.11}$$

Once these constants are found, the renormalized Z and W self-energies are given by (6.6a) with

$$\tilde{a}^{Z,W}(q^2) = a^{Z,W}(q^2) - a^{Z,W}(M_{Z,W}^2) - \delta Z_{Z,W}(q^2 - M_{Z,W}^2)\,. \tag{6.12}$$

Straightforward calculation of seven one-loop diagrams in Fig. 11 for the photon self-energy, together with (6.1) and (6.3), gives

$$\delta Z_W \sin^2\theta + \delta Z_B \cos^2\theta = \frac{e^2}{16\pi^2}\left(\frac{2}{3} + 3\ln\frac{\Lambda^2}{M_W^2} - \frac{4}{3}\sum_f Q^2 \ln\frac{\Lambda^2}{M_f^2}\right), \tag{6.13}$$

$$\begin{aligned} \tilde{\pi}^\gamma(g^2) = \frac{e^2}{16\pi^2}\Bigg\{ &-\int_0^1 dx[4 - 3(1-2x)^2]\ln\left(1 - x(1-x)\frac{q^2}{M_W^2}\right) \\ &+ 8\sum_f Q^2 \int_0^1 dx\, x(1-x)\ln\left(1 - x(1-x)\frac{q^2}{m_f^2}\right)\Bigg\}\,. \end{aligned} \tag{6.14}$$

The last term due to fermion loops is the same as in QED.

There are eleven one-loop diagrams similar to those in Fig. 11 for the Z self-energy. To see how the divergences cancel, we shall consider only the divergent terms for the moment. For a^Z in (6.4) we find

$$\begin{aligned} a^Z(g^2) \doteq \sum_{f,c}\Bigg[Z_f\left(m_f^2 - \frac{q^2}{3}\right) + 4m_f^2 \tan^2\theta Q(T_3 - Q\sin^2\theta)\Bigg]\ln\frac{\Lambda^2}{M_Z^2} \\ + [(4\cos^2\theta - 2 - \sec^2\theta)M_Z^2 + (3\cos^2\theta + \tfrac{1}{3} - \tfrac{1}{6}\sec^2\theta)q^2]\ln\frac{\Lambda^2}{M_W^2}. \end{aligned} \tag{6.15}$$

The first term is the fermion contribution; the summation is taken over flavor as well as color, and $Z_f = 2[(T_3 - Q\sin^2\theta)^2 + Q^2\sin^4\theta]/\cos^2\theta$. Calculation of 16 similar diagrams for W self-energy gives

$$a^W(q^2) \doteq \sum_{f,c}\left(\frac{m_f^2}{2} - \frac{q^2}{6}\right)\ln\frac{\Lambda^2}{M_Z^2} + [(2 - \sec^2\theta)M_W^2 + \tfrac{19}{6}q^2]\ln\frac{\Lambda^2}{M_W^2}. \tag{6.16}$$

From (5.4) and (6.10) it follows that

$$Y_{WZ} \doteq -\tfrac{1}{3}\sum_{f,c}\left[\tan^2\theta(\tfrac{1}{2} - 4Q^2\sin^2\theta)\left(\ln\frac{\Lambda^2}{M_Z^2} + \frac{5}{3}\right) + \ln\frac{M_Z^2}{M_W^2}\right] + (3\sin^2\theta + \tfrac{1}{6}\tan^2\theta)\ln\frac{\Lambda^2}{M_W^2} + \delta Y_{WZ}\,, \tag{6.17}$$

where $(g^2/16\pi^2)\delta Y_{WZ}$ is the remaining finite terms in Y_{WZ}, defined in (B3). The leading contributions of the fermions to Y_{WZ} are explicitly written in (6.17) so that the fermion contributions to δY_{WZ} are of order m_f^2/M_W^2. Numerical calculation gives

$$\delta Y_{WZ} = \begin{cases} 0.79 + 0.22 & (M_H \simeq 10\ \text{GeV}) \\ 0.79 + 0.09 & (M_H \simeq 100\ \text{GeV}) \\ 0.79 - 0.15 & (M_H \simeq 500\ \text{GeV}) \end{cases}$$

for $\sin^2\theta \simeq 0.23$ and $M_W \simeq 80$ GeV.

When the divergent terms in (6.17) are substituted in (6.11) and (6.5), all the divergent terms disappear in the renormalized functions (6.12),

$$\tilde{a}^Z(q^2) = \frac{g^2}{16\pi^2}\left\{(q^2 - M_Z^2)\left[\tfrac{4}{3}\sin^2\theta\sum_{f,c}Q^2\left(\ln\frac{M_Z^2}{m_f^2} - \frac{5}{3}\right) - \delta Y_{WZ}(\cot^2\theta - 1)\right] + \xi_Z(q^2) - \xi_Z(M_Z^2)\right\} \tag{6.18a}$$

$$\tilde{a}^W(q^2) = \frac{g^2}{16\pi^2}\left\{(q^2 - M_W^2)\sum_{f,c}\left[\tfrac{4}{3}\sin^2\theta Q^2\left(\ln\frac{M_Z^2}{m_f^2} - \frac{5}{3}\right) + \frac{\cot^2\theta - 1}{6}\ln\frac{M_Z^2}{M_W^2}\right] - (q^2 - M_W^2)\delta Y_{WZ}\cot^2\theta + \xi_W(q^2) - \xi_W(M_W^2)\right\} \tag{6.18b}$$

The functions $\xi_{Z,W}$ are given in Appendix B. Since the contribution of the longitudinal parts $\tilde{b}$ in (6.6a) to the amplitude (1.2) is zero [note $\bar{\nu}\not{q}(1-\gamma_5)\nu = 0$], we do not consider $\tilde{b}$. The contribution of (6.18) to the

amplitude (1.2) corresponding to Fig. 2(d) is

$$a_{2(d)}=c_{2(d)}=\frac{-\tilde{a}^{Z}(q^2)}{M_Z^{\,2}\left(1-\frac{q^2}{M_Z^{\,2}}\right)^2}, \tag{6.19}$$

$$b=d=0$$

We remark that, as in the case of the lepton line, the finite constants $\frac{1}{2}f_Z$ and $\frac{1}{2}f_W$ remain for the Z and W self-energies on an external line, where $f_{Z,W}$ are defined by

$$\frac{\tilde{a}^{Z,W}(q^2)}{q^2-M_{Z,W}^{\,2}}\xrightarrow[q^2\to M_{Z,W}^{\,2}]{}f_{Z,W}$$

which can be readily obtained from (6.18).

The diagrams for the Z-γ transition are exactly the same as those for the photon self-energy, Fig. 11, in which one of the external lines is replaced by a Z line. The contribution from one-loop diagrams, which we denote by $i\pi_{\mu\nu}^{Z\gamma}$, contains divergent terms, and they are canceled by the counter terms which have already been determined. To show how it works, we write the divergent terms explicitly,

$$\begin{aligned}i\pi_{\mu\nu}^{Z\gamma}\doteq{}&i(q^2g_{\mu\nu}-q_\mu q_\nu)\left[\tfrac{1}{3}\tan\theta\sum_{f,c}(\tfrac{1}{2}-4Q^2\sin^2\theta)\ln\frac{\Lambda^2}{M_Z^{\,2}}-\sin\theta(3\cos\theta+\tfrac{1}{6}\sec\theta)\ln\frac{\Lambda^2}{M_W^{\,2}}\right]\\&-ig_{\mu\nu}M_W^{\,2}\,2\sin\theta\sec\theta\ln\frac{\Lambda^2}{M_W^{\,2}}+\cdots.\end{aligned} \tag{6.20}$$

The counterterms can be found from (A6) as

$$-i(\delta Z_B-\delta Z_W)\cos\theta\sin\theta(q^2g_{\mu\nu}-q_\mu q_\nu)+i\frac{\delta g}{g}M_W^{\,2}\tan\theta\,g_{\mu\nu}. \tag{6.21}$$

From (6.17), (6.9), and (3.21), we see that the counterterms (6.21) cancel all the divergences in (6.20). Thus the renormalized Z-γ transition amplitude is given by

$$\begin{aligned}i\bar{\pi}_{\mu\nu}^{Z\gamma}(q^2)\equiv{}&i\tilde{a}^{Z\gamma}(q^2)g_{\mu\nu}+i\tilde{b}^{Z\gamma}(q^2)\frac{q_\mu q_\nu}{q^2}\\&=\frac{ig^2}{16\pi^2}(q^2g_{\mu\nu}-q_\mu q_\nu)\\&\times\Bigg(\sum_{f,c}\left\{\tan\theta(2T_3Q-4Q^2\sin^2\theta)\left[\frac{1}{3}\ln\frac{Mz^2}{m_f^{\,2}}-\frac{5}{9}-2\int_0^1dx\,x(1-x)\left(\ln\,1-x(1-x)\frac{q^2}{m_f^{\,2}}\right)\right]-\frac{\cot\theta}{6}\ln\frac{Mz^2}{M_W^{\,2}}\right\}\\&+\sin\theta\cos\theta\int_0^1dx[4-3(1-2x)^2]\ln\left(1-x(1-x)\frac{q^2}{M_W^{\,2}}\right)\\&+\tfrac{1}{2}\tan\theta\int_0^1dx(1-2x)^2\ln\left(1-x(1-x)\frac{q^2}{M_W^{\,2}}\right)-\tfrac{2}{3}\sin\theta\cos\theta+\delta Y_{WZ}\cot\theta\Bigg)\\&+\frac{ig^2}{16\pi^2}g_{\mu\nu}2M_W^{\,2}\tan\theta\int_0^1dx\ln\left(1-x(1-x)\frac{q^2}{M_W^{\,2}}\right).\end{aligned} \tag{6.22}$$

This term gives to the amplitude (1.2) the contribution, corresponding to Fig. 2(e),

$$c_{2(e)}=\frac{\cot\theta\tilde{a}^{Z\gamma}}{(1-q^2/M_Z^{\,2})q^2} \tag{6.23}$$

and $a=b=d=0$. We note that (6.22) vanishes for $q^2=0$.

VII. CORRECTIONS TO THE NEUTRAL-CURRENT AMPLITUDES

To complete the calculation box diagrams must be computed. There are four box diagrams contributing to the amplitude (1.2) as shown in Figs. 2(f) and 2(g). They are finite without subtraction. A general method of evaluation of scalar one-loop diagrams discussed by 't Hooft and Veltman[23] is useful here. Assuming $-q^2\gg m_f^{\,2}$, I find for the W-exchange box diagrams

$$\frac{-ig^2}{2M_W^{\,2}}\frac{g^2}{16\pi^2}\bar{\nu}\gamma^\alpha\frac{1-\gamma_5}{2}\nu\left[\bar{q}\gamma_\alpha(\tfrac{5}{2}T_3-\tfrac{3}{4})\frac{1-\gamma_5}{2}q\right]B(q,M_W), \tag{7.1}$$

where

$$B(q,M)=\int_0^1 dx \frac{\ln\left(1-x(1-x)\frac{q^2}{M^2}\right)-\ln x}{1-x(q^2/M^2)} \to 1 \text{ as } q^2 \to 0 . \tag{7.2}$$

As was mentioned in the Introduction, the spin terms are neglected in (7.1). Similarly, for the Z-exchange box diagrams,

$$\frac{-ig^2}{2M_Z{}^2\cos^2\theta}\frac{g^2}{16\pi^2}\bar{\nu}\gamma^\alpha\frac{1-\gamma_5}{2}\nu\bar{q}\gamma_\alpha\frac{B(q,M_Z)}{2\cos^2\theta}\left\{[\sin^2\theta(1-2\sin^2\theta)T_3-\tfrac{3}{4}(1-2\sin^2\theta+\tfrac{20}{9}\sin^4\theta)]\frac{1-\gamma_5}{2}+\sin^4\theta(Q+\tfrac{2}{3})\right\}q . \tag{7.3}$$

From (7.1) and (7.3) the box-diagram contributions to a–d, which I denote by a_{box}–d_{box}, can readily be read off.

Now we are ready to discuss the total contributions. Let us write the corrected amplitudes (1.2) as

$$T_{\text{tot}}=T_{\text{tree}}+T_{\text{weak}}+T_{\text{photon}}$$

where T_{tree} is the tree amplitude (1.1), T_{photon} is the photonic correction (4.7), and T_{weak} is the sum of all the other corrections (pure weak corrections). Since T_{photon} involves infrared divergences, one must take account of the photon bremmstrahlung corrections, the amplitude for which is denoted by T_{brems}. Thus we consider the cross section

$$d\sigma\sim|T_{\text{tree}}+T_{\text{weak}}|^2+2|T_{\text{tree}}T_{\text{photon}}|+\int|T_{\text{brems}}|^2$$

which is valid up to the order-α corrections. The last term is integrated over the photon phase space. The sum of the last two terms, which is infrared finite, represents the photonic corrections. Although in the Weinberg-Salam model electromagnetic interactions are connected with weak interactions in an essential way, the photonic correction term T_{photon} may be separated out and it has the same form as that encountered in QED. Thus the photonic corrections may be dealt with within the framework of QED, such as the analysis of the charged-current interactions considered by De Rújula, Petronzio, and Savoy-Navarro.[24] Once the data are modified for the photonic corrections, they are to be compared with the amplitude $(T_{\text{tree}}+T_{\text{weak}})$ which includes only the pure weak corrections. I now assume that the photonic corrections have been performed to the data, and discuss the weak corrections; henceforth I assume that a–d do not contain the photonic corrections (4.7).

The tree diagram and the one-loop corrections (3.27), (3.31), (4.5), (6.19), (6.23), (7.1), and (7.3) give the total contributions to a–d. Numerical calculations show that (3.31), (4.5), and (7.3) are negligible so that

$$a=\left(1-\frac{q^2}{M_Z{}^2}\right)^{-1}+a_{2(\text{d})}+a_{\text{box}},$$
$$c=\left(1-\frac{q^2}{M_Z{}^2}\right)^{-1}+c_{2(\text{a})}+c_{2(\text{d})}+c_{2(\text{e})} \tag{7.4}$$

and $b=b_{\text{box}}$, $d=d_{\text{box}}$. Numerically, $b\simeq-0.0027$ and $d\simeq0.0002$ and they are practically constant over the range $-q^2/M_W{}^2=10^{-5}-10^0$. These terms are absent in the tree approximation, but they are induced by loop diagrams. However, the results imply that the induced effects are too small to be observed, in accordance with the previous result for $q^2=0$.[25]

For small values of the momentum transfer the expressions can be written as

$$c_{2(\text{a})}\simeq\frac{g^2}{16\pi^2}\left(-\frac{16}{9}+\frac{2}{3}\ln\frac{-q^2}{M_W{}^2}\right), \tag{7.5a}$$

$$c_{2(\text{e})}\simeq\frac{g^2}{16\pi^2}\left(1-\frac{q^2}{M_Z{}^2}\right)^{-1}\left\{\sum_{f,c}\left[\tfrac{1}{3}(\tfrac{1}{2}-4Q^2\sin^2\theta)\ln\frac{M_Z{}^2}{-q^2}-\frac{\cot^2\theta}{6}\ln\frac{M_Z{}^2}{M_W{}^2}\right]-\tfrac{1}{3}-\tfrac{2}{3}\cos^2\theta+\delta Y_{WZ}\cot^2\theta\right\}, \tag{7.5b}$$

$$a_{2(\text{d})}=c_{2(\text{d})}\simeq\frac{g^2}{16\pi^2}\left(1-\frac{q^2}{M_Z{}^2}\right)^{-1}\sum_{f,c}\tfrac{4}{3}Q^2\sin^2\theta\left(\ln\frac{M_Z{}^2}{m_f{}^2}-\frac{5}{3}\right)$$
$$+\frac{g^2}{16\pi^2}\left(1-\frac{q^2}{M_Z{}^2}\right)^{-2}\left[\delta Y_{WZ}(1-\cot^2\theta)-\frac{\xi_Z(0)-\xi_Z(M_Z{}^2)}{M_Z{}^2}\right], \tag{7.5c}$$

$$a_{\text{box}}\simeq\frac{g^2}{16\pi^2}\left[\frac{5}{2}+\frac{\sin^2\theta(1-2\sin^2\theta)}{2\cos^2\theta}\right]. \tag{7.5d}$$

In (7.5b) it is assumed that $m_f^2 \ll M_Z^2$; for heavy-quark contributions one must refer to (6.22) and (6.23) instead.

The largest corrections arise from the fermion contributions in (7.5b) and (7.5c), and the estimate of the appropriate quark masses is important. The effective quark masses are known to depend on the energy, and the quark mass m_q in (7.5b) may be written as $m_q(q^2)$. We note that in (7.5c) the fermion contributions are the finite parts of the counterterms which are subtracted at $q^2 = M_Z^2$. Therefore, in (7.5c), m_q may be written as $m_q(M_Z^2)$. The values $m_q(M_Z^2)$ may be estimated from the known experimental data in the e^+e^- annihilation which measures the photon self-energy $\tilde{\Pi}^\gamma$ given by (6.14). The up-to-date dispersion calculation for $\tilde{\Pi}^\gamma$ has been performed by Paschos.[26] By identifying m_q as $m_q(q^2)$ in (6.14) and fitting the data, I find that the following values of $\tilde{\Pi}^\gamma$ in Ref. 26 with smallest errors: $m_u = m_d = 0.02$ GeV, $m_c = 2.0$ GeV, $m_s = 0.4$ GeV, $m_t = 15$ GeV, and $m_b = 5.0$ GeV for $(-q^2)^{1/2} \simeq M_{Z,W}$ (80–90 GeV). Using these values and $g^2/16\pi^2 = \alpha/4\pi \sin^2\theta = \frac{1}{396}$, I obtain the corrections which are summarized in Table I.

The smallness of the induced terms b and d allows one to write the effective neutral-current amplitude (1.2) as

$$\frac{-ig^2}{2M_Z^2 \cos^2\theta} \bar{\nu}\gamma^\alpha \frac{1-\gamma_5}{2} \nu \bar{q}\gamma_\alpha a\left(T_3 \frac{1-\gamma_5}{2} - \frac{c}{a} Q \sin^2\theta\right) q \,. \tag{7.6}$$

Our next task is to rewrite it in terms of the Fermi coupling constant G_F. To this end I write (7.6) as

$$\frac{-ig^2}{8M_W^2} \frac{M_W^2}{M_Z^2 \cos^2\theta} a \bar{\nu}\gamma^\alpha (1-\gamma_5)\nu \bar{q}\gamma_\alpha \times \left[T_3(1-\gamma_5) - \frac{c}{a} 2Q \sin^2\theta\right] q \tag{7.7}$$

TABLE I. Summary of the weak corrections in percentages. The corrections due to different values of the Higgs-boson mass M_H are given in the lower part of the table.

$(-q^2)^{1/2}$ (GeV)	$c_{2(a)}$	$c_{2(e)}$	$a_{2(d)} = c_{2(d)}$	a_{box}	$c/a - 1$	ρ_{cor}
4	−1.46	2.00	6.13	0.65	−0.11	0.34
6	−1.32	1.67	6.12	0.65	−0.30	0.09
10	−1.15	1.26	6.07	0.65	−0.54	−0.75
20	−0.92	0.71	5.86	0.65	−0.86	−4.44
M_H (GeV)						
10		0.19	−0.38		0.19	0.04
100		0.08	−0.08		0.08	0
500		−0.13	0.19		−0.13	−0.10

and consider the corrections in the following two relations

$$\frac{M_W^2}{M_Z^2 \cos^2\theta} = 1 + O(\alpha) \,, \tag{7.8a}$$

$$\frac{G_F}{\sqrt{2}} = \frac{g^2}{8M_W^2}[1 + O(\alpha)] \,. \tag{7.8b}$$

To calculate the correction term in the gauge-meson mass ratio (7.8a), let us investigate in detail the gauge-meson mass terms (2.9). Since the masses are proportional to gv, the counterterms are generated by the shift (2.8) together with $v \to v + \delta v$. Thus one must identify

$$Z_\phi M_W^2 + \delta M_W^2 = \frac{g^2 v^2}{4}\left(Z_\phi + 2\frac{\delta v}{v} + 2\frac{\delta g}{g}\right),$$

$$Z_\phi M_Z^2 + \delta M_Z^2 = \frac{g^2 v^2}{4\cos^2\theta}\left(Z_\phi + 2\frac{\delta v}{v} + 2\cos^2\theta \frac{\delta g}{g}\right),$$

which in turn give

$$\frac{M_W^2}{M_Z^2 \cos^2\theta} = 1 + \frac{\delta M_Z^2}{M_Z^2} - \frac{\delta M_W^2}{M_W^2} + 2\frac{\delta g}{g}\sin^2\theta \,. \tag{7.9}$$

The relevant counterterms are given in (3.22) and (5.4). The last term involving δg in (7.9) just cancels the divergences in the first two mass counterterms, and the total contribution is finite. Numerically the correction is small; I find

$$\frac{M_W^2}{M_Z^2 \cos^2\theta} \equiv 1 + \delta_M = \begin{cases} 1.0011 + 0.0004 & (M_H = 10 \text{ GeV}) \\ 1.0011 - 0.0001 & (M_H = 100 \text{ GeV}) \,. \\ 1.0011 - 0.0010 & (M_H = 500 \text{ GeV}) \end{cases} \tag{7.10}$$

Note that fermions have no effect on this relation [see Appendix C].

Next we consider the corrections in the relation (7.8b) which is given by the muon decay amplitude. The radiative corrections to the muon decay amplitude in the Weinberg-Salam model have been calculated in Refs. 8, 11, and 12, and we refer to the work of Ross[11] who has used the same renormalization procedure as the one employed here. The result may be summarized as in the following form for the amplitude

$$\frac{-ig^2}{8M_W^2} \bar{\nu}_\mu \gamma^\alpha (1-\gamma_5)\mu \bar{e}\gamma_\alpha (1-\gamma_5)\nu_e \left(1 + \frac{-\tilde{a}^W(0)}{M_W^2} + \eta + R\right). \tag{7.11}$$

The term $-\tilde{a}^W(0)/M_W^2$ represents the W self-energy contribution, where $\tilde{a}^W(0)$ is given by (6.18b) with $q^2 = 0$. Note that $\tilde{a}^W$ is infrared finite. The constant η contains all the vertex corrections, and box-diagram contributions that do not involve

photon exchanges. Note that η is also infrared finite. The box-diagram contributions to η are negligible while the vertex corrections give $\eta \simeq -0.005$. The term R contains all the photonic corrections arising from the photon exchange in box diagrams and the factor f_L given in (3.13). It turns out that R is exactly the same as the photonic corrections encountered in the current-current interaction theory.[11] Therefore one must identify

$$\frac{G_F}{\sqrt{2}} = \frac{g^2}{8M_W^2}(1+\delta_\mu) \equiv \frac{g^2}{8M_W^2}\left(1 + \frac{-\tilde{a}^W(0)}{M_W^2} + \eta\right). \quad (7.12)$$

The W self-energy contribution is given by

$$\frac{-\tilde{a}^W(0)}{M_W^2} = \frac{g^2}{16\pi^2}\left\{\sum_{f,c}\left[\tfrac{4}{3}Q^2\sin^2\theta\left(\ln\frac{M_Z^2}{m_f^2} - \frac{5}{3}\right) + \frac{\cot^2\theta - 1}{6}\ln\frac{M_Z^2}{M_W^2}\right] - \delta Y_{WZ}\cot^2\theta - \frac{\xi_W(0) - \xi_W(M_W^2)}{M_W^2}\right\}. \quad (7.13)$$

Using the effective values for $m_q(M_W^2) \simeq m_q(M_Z^2)$ given above, I find

$$\delta_\mu = 0.0635\begin{cases} -0.0037 & (M_H = 10\ \text{GeV}) \\ -0.0009 & (M_H = 100\ \text{GeV}) \\ +0.0021 & (M_H = 500\ \text{GeV}) \end{cases}. \quad (7.14)$$

Using the results (7.10) and (7.14) the amplitudes may be written as

$$\frac{-iG_F}{\sqrt{2}}\rho\bar{\nu}\gamma^\alpha(1-\gamma_5)\nu\bar{q}\gamma_\alpha\left[T_3(1-\gamma_5) - \frac{c}{a}2Q\sin^2\theta\right]q. \quad (7.15)$$

In the tree approximation with $q^2 = 0$ we have $\rho = 1$ and $c/a = 1$. The corrections $\rho_{\text{cor}} = \rho - 1$ and $(a/c - 1)$ are listed in Table I for various values of $(-q^2)^{1/2}$. If the amplitudes (1.2) are parametrized as[1]

$$\frac{-iG_F}{\sqrt{2}}\bar{\nu}\gamma^\alpha(1-\gamma_5)\nu\{\bar{u}\gamma_\alpha[u_L(1-\gamma_5) + u_R(1+\gamma_5)]u + \bar{d}\gamma_\alpha[d_L(1-\gamma_5) + d_R(1+\gamma_5)]d\}, \quad (7.16)$$

the parameters $u_{L,R}$ and $d_{L,R}$ are given by

$$\begin{aligned} u_L &= \tfrac{1}{2}\rho - \tfrac{2}{3}\rho\frac{c}{a}\sin^2\theta, \\ d_L &= -\tfrac{1}{2}\rho + \tfrac{1}{3}\rho\frac{c}{a}\sin^2\theta, \\ u_R &= -\tfrac{2}{3}\rho\frac{c}{a}\sin^2\theta, \\ d_R &= -\tfrac{1}{3}\rho\frac{c}{a}\sin^2\theta. \end{aligned} \quad (7.17)$$

In this parametrization the effect of the weak corrections are small in the neutral-current interactions. However, this is so if one uses the definition of $\sin^2\theta$ as defined here, but the radiative corrections can in principle be larger for $\sin^2\theta$ defined in some other way.

The smallness of the corrections is due to the cancellation between similar contributions of the Z and W self-energies in (7.5c) and (7.11). Therefore a large correction is expected where they do not cancel. One such example is the prediction of the gauge-meson masses. In fact, Marciano has shown[27] by renormalization-group arguments that the gauge-meson masses are modified from the naive values by ~+3%. Subsequently, Sirlin has shown[28] that the mass correction in the one-loop approximation is a 3.3% increase. Since our definition of $\sin^2\theta$ is slightly different from Sirlin's, I calculate, for completeness, the mass corrections using (7.10), (7.14), $g^2 = 4\pi\alpha/\sin^2\theta$, and the value $G_F = 1.166 \times 10^{-5}\ \text{GeV}^{-2}$.[29] The 6.4% correction in (7.14) implies the mass correction of 3.2%, in agreement with Refs. 27 and 28. The values of M_W and M_Z for various values of $\sin^2\theta$ are listed in Table II. Similar calculations are also performed by Veltman, and Antonelli, Consoli, and Corbó,[30] who found somewhat larger corrections to the gauge-meson masses, 3.7–4.7%. Their results are in apparent contradiction with that of Refs. 27 and 28 and ours, but a direct comparison would be misleading because of the different renormalization methods used. Their $\sin^2\theta$ may involve also a large correction which cancels a part of the mass corrections. In our treatment it is clear how to extract $\sin^2\theta$ from neutral-cur-

TABLE II. The gauge-meson masses in GeV. The corrections due to different Higgs-boson masses are given in the lower part of the table.

$\sin^2\theta$	M_W	M_Z
0.220	82.03	92.78
0.225	81.12	92.04
0.230	80.23	91.32
0.235	79.37	90.64
0.240	78.54	89.99
M_H (GeV)		
10	−0.15	−0.19
100	−0.03	−0.04
500	+0.08	+0.15

rent experiments, which then predicts the gauge-meson masses as in Table II.

Note added in proof. After this paper was submitted, corrections to the work of Ref. 30 appeared [M. Green and M. Veltman, Nucl. Phys. B175, 547 (1980); F. Antonelli *et al.*, Phys. Lett. (to be published)]. Their results on the gauge-boson mass shift are now consistent with those of Refs. 27 and 28, and ours.

ACKNOWLEDGMENTS

I wish to thank L. M. Sehgal for numerous discussions and encouragement and E. A. Paschos for discussions and suggestions.

APPENDIX A: LAGRANGIANS

We give the expressions for the Lagrangian (2.5),

$$\mathcal{L}_l = \bar{\nu}_l i\partial\!\!\!/ \nu_l + \bar{l}(i\partial\!\!\!/ - m_l)l + e\bar{l}\gamma^\mu l A_\mu + \frac{g}{\sqrt{2}}(\nu_l\gamma^\mu l_L W_\mu^+ + \bar{l}_L\gamma^\mu\nu_l W_\mu^-) + \frac{g}{2\cos\theta}\bar{\nu}_l\gamma^\mu\nu_l Z_\mu$$
$$+\left(-\frac{g\cos 2\theta}{2\cos\theta}\bar{l}_L\gamma^\mu l_L + \frac{g\sin^2\theta}{\cos\theta}\bar{l}_R\gamma^\mu l_R\right)Z_\mu - \frac{g}{\sqrt{2}}\frac{m_l}{M_W}(\bar{\nu}_l l_R\phi^+ + \bar{l}_R\nu_l\phi^-) - \frac{g}{2}\frac{m_l}{M_W}(\bar{l}l\psi + i\bar{l}\gamma_5 l\chi)\,, \tag{A1}$$

$$\mathcal{L}_{II} = -\tfrac{1}{2}\left|\partial_\mu W_\nu^+ - \partial_\nu W_\mu^+ - ie(W_\mu^+ A_\nu - W_\nu^+ A_\mu) + ig\cos\theta(W_\mu^+ Z_\nu - W_\nu^+ Z_\mu)\right|^2$$
$$-\tfrac{1}{4}[\partial_\mu Z_\nu - \partial_\nu Z_\mu + ig\cos\theta(W_\mu^- W_\nu^+ - W_\mu^+ W_\nu^-)]^2 - \tfrac{1}{4}[\partial_\mu A_\nu - \partial_\nu A_\mu - ie(W_\mu^- W_\nu^+ - W_\mu^+ W_\nu^-)]^2\,, \tag{A2}$$

$$\mathcal{L}_{III} = \left|\partial_\mu\phi^+ - ig\frac{\cos 2\theta}{2\cos\theta}Z_\mu\phi^+ + ieA_\mu\phi^+ - iM_W W_\mu^+ - \frac{i}{2}gW_\mu^+(\psi + i\chi)\right|^2$$
$$+\tfrac{1}{2}\left|\partial_\mu(\psi + i\chi) - igW_\mu^-\phi^+ + iM_Z Z_\mu + \frac{ig}{2\cos\theta}Z_\mu(\psi + i\chi)\right|^2\,, \tag{A3}$$

$$\mathcal{L}_{IV} = -\tfrac{1}{2}M_H{}^2\psi^2 - \frac{gM_H{}^2}{2M_W}\chi(\phi^+\phi^- + \tfrac{1}{2}|\psi + i\chi|^2) - \frac{g^2M_H{}^2}{8M_W{}^2}(\phi^+\phi^- + \tfrac{1}{2}|\psi + i\chi|^2)^2\,. \tag{A4}$$

The Faddeev-Popov ghost Lagrangian is

$$\mathcal{L}_{FP} = -\bar{c}^+(\partial^2 + M_W{}^2)c^+ + ig\cos\theta\bar{c}^+\partial^\mu(Z_\mu c^+) - ie\bar{c}^+\partial^\mu(A_\mu c^+) - ig\bar{c}^+\partial^\mu[W_\mu^+(c_Z\cos\theta - c_A\sin\theta)]$$
$$-M_W\bar{c}^+\left[\frac{g\cos 2\theta}{2\cos\theta}c_Z\phi^+ - ec_A\phi^+ + \frac{g}{2}c^+(\psi + i\chi)\right] + [c^+ \to c^-,\ W^+ \to W^-,\ i \to -i]$$
$$-\bar{c}_Z(\partial^2 + M_Z{}^2)c_Z - ig\cos\theta\bar{c}_Z\partial^\mu(c^+W_\mu^- - c^-W_\mu^+) - M_Z\bar{c}_Z\left(-\frac{g}{2}c^-\phi^+ - \frac{g}{2}c^+\phi^- + \frac{g}{2\cos\theta}c_Z\psi\right)$$
$$-\bar{c}_A\partial^2 c_A + ie\bar{c}_A\partial^\mu(c^+W_\mu^- - c^-W_\mu^+)\,. \tag{A5}$$

The relevant terms in the counterterm Lagrangian are

$$\mathcal{L}_{WS}^c = \delta Z_L\bar{\nu}i\partial\!\!\!/\nu + \delta Z_L\bar{l}_L i\partial\!\!\!/ l_L + \delta Z_R\bar{l}_R i\partial\!\!\!/ l_R - \delta m\bar{l}l + \left(\frac{g}{2\cos\theta}\delta Z_L + \frac{\delta g}{2}\cos\theta\right)\bar{\nu}\gamma^\mu\nu Z_\mu - \frac{\delta g}{2}\sin\theta\bar{\nu}\gamma^\mu\nu A_\mu$$
$$-\bar{l}\gamma^\mu\left[\left(\frac{g\cos 2\theta}{2\cos\theta}\delta Z_L + \frac{\delta g}{2}\cos\theta\right)\frac{1-\gamma_5}{2} + g\frac{\sin^2\theta}{\cos\theta}\delta Z_R\frac{1+\gamma_5}{2}\right]lZ_\mu$$
$$-\bar{l}\gamma^\mu\left[\left(e\delta Z_L + \frac{\delta g}{2}\sin\theta + \frac{\delta g'}{2}\cos\theta\right)\frac{1-\gamma_5}{2} + \left(e\delta Z_R + \delta g'\cos\theta\right)\frac{1+\gamma_5}{2}\right]lA_\mu + \frac{g}{\sqrt{2}}\left(\delta Z_L + \frac{\delta g}{g}\right)(\bar{\nu}\gamma^\mu l_L W_\mu^+ + \bar{l}_L\gamma^\mu\nu W_\mu^-)$$
$$-\tfrac{1}{2}\delta Z_W\left|\partial_\mu W_\nu^+ - \partial_\nu W_\mu^+\right|^2 + (\delta Z_\phi M_W{}^2 + \delta M_W{}^2)W_\mu^+ W^{-\mu} - \tfrac{1}{4}(\delta Z_W\sin^2\theta + \delta Z_B\cos^2\theta)(\partial_\mu A_\nu - \partial_\nu A_\mu)^2$$
$$-\tfrac{1}{4}(\delta Z_W\cos^2\theta + \delta Z_B\sin^2\theta)(\partial_\mu Z_\nu - \partial_\nu Z_\mu)^2 + \tfrac{1}{2}(\delta Z_\phi M_Z{}^2 + \delta M_Z{}^2)Z_\mu Z^\mu$$
$$-\tfrac{1}{2}(\delta Z_B - \delta Z_W)\cos\theta\sin\theta(\partial_\mu Z_\nu - \partial_\nu Z_\mu)(\partial^\mu A^\nu - \partial^\nu A^\mu) + \frac{\delta g}{g}M_W{}^2\frac{\sin\theta}{\cos\theta}Z_\mu A^\mu + \cdots\,. \tag{A6}$$

APPENDIX B: THE FUNCTIONS $\xi_{z,w}$

The function ξ_W is given by

$$\xi_W(q^2) = q^2\sum{}'\left[\tfrac{5}{9} + 2\int_0^1 dx\,x(1-x)\ln\left(x\frac{m_+{}^2}{M_W{}^2} + (1-x)\frac{m_-{}^2}{M_W{}^2} - x(1-x)\frac{q^2}{M_W{}^2}\right)\right] + q^2(-\tfrac{5}{12} + \cos^2\theta)$$
$$-\tfrac{1}{2}\int_0^1 dx[(x-2)M_W{}^2 + (1-x)M_H{}^2 - x(1-x)q^2]\ln\left(x + (1-x)\frac{M_H{}^2}{M_W{}^2} - x(1-x)\frac{q^2}{M_W{}^2}\right)$$
$$-\cos^2\theta\int_0^1 dx\{q^2[4 - 3(1-2x)^2] - 4q^2(1-2x) + 6(M_W{}^2 - M_Z{}^2)(1-x)\}\ln\left(x + (1-x)\frac{M_Z{}^2}{M_W{}^2} - x(1-x)\frac{q^2}{M_W{}^2}\right)$$

$$+(\tfrac{1}{4}-\cos^2\theta)\int_0^1 dx[q^2(1-2x)^2+q^2(1-2x)-2(M_W{}^2-M_Z{}^2)(1-x)]\ln\left(x+(1-x)\frac{M_Z{}^2}{M_W{}^2}-x(1-x)\frac{q^2}{M_W{}^2}\right)$$
$$-M_W{}^2\left(\cos^2\theta+2-\frac{1}{\cos^2\theta}\right)\int_0^1 dx\ln\left(x+(1-x)\frac{M_Z{}^2}{M_W{}^2}-x(1-x)\frac{q^2}{M_W{}^2}\right)$$
$$-\sin^2\theta\int_0^1 dx[5(1-2x+2x^2)q^2+(8x-1)M_W{}^2]\ln\left(x+(1-x)\frac{\delta^2}{M_W{}^2}-x(1-x)\frac{q^2}{M_W{}^2}\right), \tag{B1}$$

where the summation $\sum'$ is taken over fermion doublets and color, and $m_\pm$ is the mass of the $T_3=\pm\frac{1}{2}$ fermion.

The function ξ_Z is given by

$$\xi_Z(q^2)=q^2\sum_{f,c}' Z_f\left[\tfrac{5}{9}+2\int_0^1 dx\,x(1-x)\ln\left(\frac{m_f{}^2}{M_Z{}^2}-x(1-x)\frac{q^2}{M_Z{}^2}\right)\right]+q^2\left(\tfrac{2}{3}\cos^2\theta-\frac{1}{12\cos^2\theta}\right)$$
$$-\frac{1}{2\cos^2\theta}\int_0^1 dx[(x-2)M_Z{}^2+(1-x)M_H{}^2-x(1-x)q^2]\cdot\ln\left(x+(1-x)\frac{M_H{}^2}{M_Z{}^2}-x(1-x)\frac{q^2}{M_Z{}^2}\right)$$
$$-q^2\cos^2\theta\int_0^1 dx[4-3(1-2x)^2]\ln\left(1-x(1-x)\frac{q^2}{M_W{}^2}\right)$$
$$+q^2\left(\frac{1}{4\cos^2\theta}-1\right)\int_0^1 dx(1-2x)^2\ln\left(1-x(1-x)\frac{q^2}{M_W{}^2}\right)$$
$$-\left(4-\frac{2}{\cos^2\theta}\right)M_W{}^2\int_0^1 dx\ln\left(1-x(1-x)\frac{q^2}{M_W{}^2}\right). \tag{B2}$$

δY_{WZ} is given by

$$\delta Y_{WZ}=3\sin^2\theta+\frac{\tan^2\theta}{4}+\left(\frac{1}{4}\frac{M_H{}^2}{M_W{}^2}-3-\frac{1}{2\cos^2\theta}\right)\ln\frac{M_Z{}^2}{M_W{}^2}$$
$$+\frac{\xi_W(M_W{}^2)}{M_W{}^2}-\frac{\xi_Z(M_Z{}^2)}{M_Z{}^2}+\frac{16\pi^2}{g^2}\left(\frac{\delta M_W{}^2}{M_W{}^2}-\frac{\delta M_Z{}^2}{M_Z{}^2}\right)+4\sin^2\theta\ln\frac{\Lambda^2}{M_W{}^2}. \tag{B3}$$

Numerically we have

$$\frac{\xi_W(0)-\xi_W(M_W{}^2)}{M_W{}^2}=-2.616\begin{cases}+0.729 & (M_H=10\text{ GeV})\\ +0.047 & (M_H=100\text{ GeV})\\ -0.311 & (M_H=500\text{ GeV})\end{cases}$$

$$\frac{\xi_Z(0)-\xi_Z(M_Z{}^2)}{M_Z{}^2}=-1.453\begin{cases}+0.985 & (M_H=10\text{ GeV})\\ +0.110 & (M_H=100\text{ GeV})\\ -0.373 & (M_H=500\text{ GeV})\end{cases} \tag{B4}$$

APPENDIX C: GENERAL FEATURES OF THE RADIATIVE CORRECTIONS

As is mentioned in the Introduction, the advantage of the calculations of loop diagrams in a renormalizable gauge is that the contribution of each diagram such as the one in Fig. 2 may be separately considered, since all Green's functions are finite after renormalization in such a gauge. The problem of gauge invariance is more subtle because the contribution of each diagram depends on gauge reflecting the gauge dependence of the corresponding Green's function, although the gauge invariance of the total contribution is of course guaranteed. However, the difference in gauge appears in the difference in the longitudinal components of the gauge-meson propagators, which in turn give rise to a difference of the order $G_F\alpha(m_f{}^2/M_W{}^2)$ for each diagram in Fig. 2. Thus the gauge dependence does not affect the contribution of each diagram up to the order $G_F\alpha$, and therefore the discussion of the general properties of each diagram is meaningful. We now concentrate on the 't Hooft–Feynman gauge.

Let us first summarize the general properties of the vertex corrections.

(1) The photonic corrections at the $\bar{f}f\gamma$ vertex or $\bar{f}fZ$ vertex are the same as those in QED; the tree-diagram term times the infrared-divergent function which appears also in QED, as in (4.7).

(2) The W and/or Z contributions to the $\bar{f}f\gamma$ or $\bar{f}fZ$ vertices are proportional to $q^2/M_W{}^2$ for not too large q^2, after renormalization. Therefore, for $|q^2|/M_W{}^2\ll 1$ the contribution is very small. This is in fact the content of the heavy-particle decoupling of the Appelquist-Carazzone theorem.[31]

(3) The above remark does not apply to the $\bar{\nu}\nu\gamma$ vertex in Fig. 2(a). Although it is proportional to $q^2/M_W{}^2$, the factor q^2 is just canceled by q^{-2} in the photon propagator, so that the contribution does not decouple for $|q^2|\ll M_W{}^2$.

(4) The correction at the $\bar{f}fW$ ($\bar{\nu}lW$) vertex does

not vanish at $q^2=0$, though numerically it is small, 0.25%. The q^2-dependent terms are again proportional to $q^2/M_W{}^2$ for small q^2. An important point is that this vertex function is infrared finite except at $q^2=M_W{}^2$. Therefore its contribution to the muon decay amplitude, for which $q^2\simeq 0$, is infrared finite.

Next we consider the gauge-meson self-energy corrections and the propagators.

(5) The photon self-energy has been subtracted on shell of the photon. Therefore it has the form $(q^2q_{\mu\nu}-q_\mu q_\nu)\tilde{\pi}^\gamma(q^2)$ with $\tilde{\pi}^\gamma(0)=0$. In particular, the W-meson contribution to $\tilde{\pi}^\gamma$ is suppressed by the factor $q^2/M_W{}^2$ for small q^2. It is again justified by the Appelquist-Carazzone theorem.

(6) The W and Z self-energies are subtracted on shell of the corresponding particles. This implies that the renormalized W and Z propagators are proportional, in the $q^2\to 0$ limit, to $[1+O(\alpha)]/M_{W,Z}{}^2$, where the $O(\alpha)$ are given by $-\tilde{a}^{W,Z}(0)/M_{W,Z}{}^2$.

Since these correction terms gave rise to the largest effects, let us discuss them in some detail. We simplify the argument by considering a case of a neutral scalar with mass M, which is free from complications due to the Lorentz and isospin indices. Let $\pi(q^2)$ be the renormalized self-energy which is obtained by subtracting counterterms from the corresponding unrenormalized self-energy. Then the renormalized propagator $\Delta_R(q^2)$ is proportional to $[q^2-M^2-\pi(q^2)]^{-1}$. We discuss two different choices for the subtraction points.

(a) Subtraction on shell, $q^2=M^2$. The counterterms are chosen so that $\pi(M^2)=0$. Therefore $\Delta_R(q^2)$ has a pole at $q^2=M^2$. This means that M is the physical mass. In the limit $q^2\to 0$ we have $\Delta_R(0)\propto[-M^2-\pi(0)]^{-1}\simeq-[1-\pi(0)/M^2]/M^2$ which is to be compared with $-1/M^2$ in the tree approximation. The term $-\pi(0)/M^2$ is the $O(\alpha)$ term mentioned in (6) above.

(b) Subtraction at $q^2=0$. The counterterms are chosen so that $\pi(0)=0$. Then $\Delta_R(q^2)$ has a pole at $q^2=\bar{M}^2$, where $\bar{M}$ is determined by the equation $\bar{M}^2-M^2-\pi(\bar{M}^2)=0$. Thus $\bar{M}$ is the physical mass, but M is not. The M is a parameter that characterizes the theory and it is related to the physical mass by the above equation. In the limit $q^2\to 0$ we have $\Delta_R(0)\propto -1/M^2$ which is the same as that in the tree approximation.

Of course these two methods are physically equivalent; when an amplitude is expressed in terms of physical quantities both methods give the same result.

Let us compare these two methods in the calculation of the radiative correction to the muon decay amplitude. Appelquist *et al.*[8] have employed the dispersion method. The W self-energy is divergent and therefore requires a subtraction. However, when the self-energy is embedded in the amplitude as in Fig. 2(d), the absorptive part of the amplitude becomes apparently less divergent due to the extra denominators of the propagators. The amplitude is then obtained by dispersing the absorptive part without subtraction. The resultant amplitude is proportional to $-1/M_W{}^2$ in the $q^2\to 0$ limit. This procedure therefore corresponds to the subtraction at $q^2=0$ for the W self-energy, the case (b) above. Although this correction looked apparently small, a large correction arises if the amplitude is expressed in terms of the physical W mass. This point is not discussed in Ref. 8. On the other hand, Ross[11] has used method 6(a) so that the mass is the physical one while the amplitude received the large correction from the W self-energy.

Finally I remark that in method (a) employed in this paper, the gauge-meson mass counterterms are calculated from the self-energies of the FP ghosts. This is dictated solely by the gauge invariance, and since the FP ghosts do not couple to fermions there is no fermion contribution to the mass counterterms. This does not mean, however, that fermions do not contribute to the mass shift. In fact, the fermions give the dominant terms in $\tilde{a}^W(0)$ which in turn gives rise to the ~3% increase in the gauge-meson masses from the naive predictions, as is discussed in Sec. VII.

[1]L. M. Sehgal, in *Neutrinos—78*, proceedings of the International Conference on Neutrino Physics and Astrophysics, Purdue Univ., edited by E. C. Fowler (Purdue University Press, West Lafayette, Indiana, 1978).

[2]S. Weinberg, Phys. Rev. Lett. 19, 1264 (1967); A. Salam, in *Elementary Particle Theory: Relativistic Groups and Analyticity (Nobel Symposium No. 8)*, edited by N. Svartholm (Almqvist and Wiksell, Stockholm, 1968), p. 367.

[3]C. Baltay, in *Proceedings of the 19th International Conference on High Energy Physics, Tokyo, 1978*, edited by S. Homma, M. Kawaguchi, and H. Miyazawa (Physical Society of Japan, Tokyo, 1979), p. 882; F. Dydak, European Physical Society International Conference on High Energy Physics, Geneva, Switzerland, 1979 (unpublished).

[4]W. A. Bardeen, R. Gastmans, and B. Lautrup, Nucl. Phys. B46, 319 (1972); Z. Z. Aydin, S. A. Baran, and A. O. Barut, *ibid.* B55, 601 (1973).

[5]T. Appelquist and H. Quinn, Phys. Lett. 39B, 229 (1972); S. Y. Lee, Phys. Rev. D 6, 1701 (1972); G. Rajasekaran, *ibid.* 6, 3032 (1972); S. A. Baran, Nucl. Phys. B62, 333 (1973).

[6]K. Fujikawa, B. W. Lee, and A. I. Sanda, Phys. Rev.

D 6, 2923 (1972).
[7]G. 't Hooft, Nucl. Phys. B35, 167 (1971).
[8]T. W. Appelquist, J. R. Primack, and H. R. Quinn, Phys. Rev. D 6, 2998 (1972); 7, 2998 (1973).
[9]C. Bollini, J. Giambiagi and A. Sirlin, Nuovo Cimento 16A, 423 (1973); W. J. Marciano, Nucl. Phys. B84, 132 (1975); P. Salomonson and Y. Ueda, Phys. Rev. D 11, 2606 (1975).
[10]D. A. Ross and J. C. Taylor, Nucl. Phys. B51, 125 (1973); B58, 643(E) (1973).
[11]D. A. Ross, Nucl. Phys. B51, 116 (1973).
[12]G. Passarino and M. Veltman, Nucl. Phys. B160, 151 (1979); M. Lemoine and M. Veltman, *ibid.* B165, 445 (1980); M. Green and M. Veltman, Utrecht report, 1980 (unpublished).
[13]L. D. Faddeev and V. N. Popov, Phys. Lett. 25B, 29 (1967); B. W. Lee, *ibid.* 46B, 214 (1973).
[14]G. 't Hooft and M. Veltman, Nucl. Phys. B44, 189 (1972).
[15]M. Chanowitz, M. Furman, and I. Hinchliffe, Nucl. Phys. B159, 225 (1979), and references therein.
[16]Appelquist, Primack, and Quinn, the first paper in Ref. 8; Passarino and Veltman, the first paper in Ref. 12.
[17]The notation $\delta Z = Z - 1$ is used for all wave-function renormalization constants.
[18]S. Sakakibara and L. M. Sehgal, Phys. Lett. 83B, 77 (1979).
[19]I am grateful to Mr. J. Cole who pointed out a numerical error in (3.26) in the earlier version.
[20]E. S. Abers and B. W. Lee, Phys. Rep. C9, 1 (1973).
[21]This fact becomes clear by the algebraic manipulation used by R. N. Mohapatra, S. Sakakibara, and J. Sucher, Phys. Rev. D 10, 1844 (1974).
[22]This may not be clear in the usual path-integral approach, but this can be justified by the canonical method of T. Kugo and I. Ojima, Phys. Lett. 73B, 459 (1978).
[23]G. 't Hooft and M. Veltman, Nucl. Phys. B153, 365 (1979).
[24]A. De Rujula, R. Petronzio, and A. Savoy-Navarro, Nucl. Phys. B154, 394 (1979).
[25]R. N. Mohapatra and G. Senjanović, Phys. Rev. D 19, 2165 (1979). Similar calculations involving box diagrams are discussed in W. J. Marciano and A. I. Sanda, Phys. Rev. D 17, 3055 (1978).
[26]E. A. Paschos, Nucl. Phys. B159, 285 (1979).
[27]W. J. Marciano, Phys. Rev. D 20, 274 (1979).
[28]A. Sirlin, Phys. Rev. D 22, 971 (1980).
[29]R. E. Shrock, and L.-L. Wang, Phys. Rev. Lett. 41, 1692 (1978).
[30]M. Veltman, Phys. Lett. 91B, 95 (1980); F. Antonelli, M. Consoli, and G. Corbó, *ibid.* 91B, 90 (1980).
[31]T. Appelquist, and J. Carazzone, Phys. Rev. D 11, 2856 (1975).